



HAL
open science

The Influence of Carbonate Platforms on the Geomorphological Development of a Mixed Carbonate-Siliciclastic Margin (Great Barrier Reef, Australia)

Amanda Thran, Madison East, Jody Webster, Tristan Salles, Carole Petit

► **To cite this version:**

Amanda Thran, Madison East, Jody Webster, Tristan Salles, Carole Petit. The Influence of Carbonate Platforms on the Geomorphological Development of a Mixed Carbonate-Siliciclastic Margin (Great Barrier Reef, Australia). *Geochemistry, Geophysics, Geosystems*, 2020, 21 (4), pp.e2020GC008915. 10.1029/2020GC008915 . hal-02975991

HAL Id: hal-02975991

<https://hal.science/hal-02975991>

Submitted on 20 Apr 2021

HAL is a multi-disciplinary open access archive for the deposit and dissemination of scientific research documents, whether they are published or not. The documents may come from teaching and research institutions in France or abroad, or from public or private research centers.

L'archive ouverte pluridisciplinaire **HAL**, est destinée au dépôt et à la diffusion de documents scientifiques de niveau recherche, publiés ou non, émanant des établissements d'enseignement et de recherche français ou étrangers, des laboratoires publics ou privés.

Geochemistry, Geophysics, Geosystems

RESEARCH ARTICLE

10.1029/2020GC008915

Key Points:

- Platforms exert fundamental control on the development of paleochannels, fluvial mounds, shelf-edge deltas, submarine canyons, and basin flows
- Carbonate platforms obstruct/re-route lowstand rivers and promote turbidity current-driven incision of submarine canyons
- Simulations indicate that when platforms are absent, many features are not reproduced, and a “reciprocal” model of sedimentation dominates

Supporting Information:

- Supporting Information S1

Correspondence to:

A. C. Thran,
amanda.thran@sydney.edu.au

Citation:

Thran, A. C., East, M., Webster, J. M., Salles, T., & Petit, C. (2020). The influence of carbonate platforms on the geomorphological development of a mixed carbonate-siliciclastic margin (Great Barrier Reef, Australia). *Geochemistry, Geophysics, Geosystems*, 21, e2020GC008915. <https://doi.org/10.1029/2020GC008915>

Received 10 JAN 2020

Accepted 13 MAR 2020

Accepted article online 16 MAR 2020

The Influence of Carbonate Platforms on the Geomorphological Development of a Mixed Carbonate-Siliciclastic Margin (Great Barrier Reef, Australia)

Amanda C. Thran^{1,2} , Madison East², Jody M. Webster² , Tristan Salles^{1,2} , and Carole Petit³

¹EarthByte Group, School of Geosciences, The University of Sydney, Sydney, New South Wales, Australia, ²Geocoastal Research Group, School of Geosciences, The University of Sydney, Sydney, New South Wales, Australia, ³Université Côte d'Azur, CNRS, Observatoire de la Côte d'Azur, IRD, Géoazur, Valbonne, France

Abstract Sedimentation regimes on the Great Barrier Reef margin often do not conform to more conventional sequence stratigraphic models, presenting difficulties when attempting to identify key processes that control the margin's geomorphological evolution. By obstructing and modifying down-shelf and down-slope flows, carbonate platforms are thought to play a central role in altering the distribution and morphological presentation of common margin features. Using numerical simulations, we test the role of the carbonate platforms in reproducing several features (i.e., paleochannels, shelf-confined fluvial sediment mounds, shelf-edge deltas, canyons, and surface gravity flows) that have been described from observational data (seismic sections, multibeam bathymetry, sediment cores, and backscatter imagery). When carbonate platforms are present in model simulations, several notable geomorphological features appear, especially during lowstand. Upon exposure of the shelf, platforms reduce stream power, promoting mounding of fluvial sediments around platforms. On the outer shelf, rivers and streams are re-routed and coalesce between platforms, depositing shelf-edge deltas and incising paleochannels through knickpoint retreat. Additionally, steep platform topography triggers incision of slope canyons through turbidity currents, and platforms act as conduits for the localized delivery of land and shelf-derived sediments to the continental slope and basin. When platforms are absent from the topographic surface, the model is unable to reproduce many of these features. Instead, a more typical “reciprocal-type” sedimentation regime arises. Our results demonstrate the essential role of carbonate platform topography in modulating key bedload processes. Therefore, they exert direct control on the development of various geomorphological features within the shelf, slope, and basin environments.

Plain Language Summary The modern Great Barrier Reef sits atop the skeletal remains of its ancestors. These remains form large (50–200 km²) columns of chalk (or carbonate platforms) that rest on the northeast Australian continental shelf. By comparing observational data with computer simulations, we find that these platforms majorly disrupt and modify the flow of rivers and deep-sea density currents during periods of lower sea level. When platforms are exposed, they become hills, forming steep topographic high points that are large enough to re-route rivers and promote incision on the continental slope. On the modern seafloor, evidence of this activity is preserved in the form of ancient deltas, paleochannels, submarine canyons, and sediment flows that stretch across the abyssal plain. The morphology and distribution of these seafloor features are more robustly accounted for when carbonate platforms are present, and many of them do not appear in computer simulations where carbonate platforms are absent. Our work shows that carbonate platforms can alter seascapes in ways that are traditionally less understood.

1. Introduction

Submarine geomorphology provides a crucial window into the myriad of hydrodynamic, sedimentary, biological, and climatic processes that operate on continental margins over geological timescales. The processes that form features such as paleochannels, submarine canyons, sediment gravity flows, and submarine fans are well understood within a typical sequence stratigraphic framework, which heavily emphasizes the role of eustatic sea level position in mediating source-to-sink sediment transport in what are typically

siliciclastic-dominated depositional settings (Emery & Myers, 2009; Jervey, 1988; Posamentier et al., 1988; van Wagoner et al., 1988). In carbonate-dominated settings (e.g., warm and cool water “carbonate factories”), sequence stratigraphic models mainly focus on the geomorphological development of carbonate platforms (Eberli & Ginsburg, 1989; Kendall & Schlager, 1981; Sarg, 1988). Australia’s Great Barrier Reef margin is the world’s largest extant mixed carbonate-siliciclastic system, and while it hosts many features that are ubiquitous in both siliciclastic- and carbonate-dominated settings, the margin repeatedly deviates from conventional styles of geomorphological development that are predicted by these end-member scenarios (Dunbar et al., 2000; Dunbar & Dickens, 2003b).

At the heart of these discrepancies, carbonate platforms are largely speculated to play a role, where platforms interrupt and modify typical cross-shelf and downslope sediment transport (Dunbar et al., 2000; Dunbar & Dickens, 2003b; Fielding et al., 2003; Page & Dickens, 2005). On the inner to mid-continental shelf, paleochannels, which are typically incised by rivers during eustatic lowstands, appear to be discontinuous and shallow in seismic sections, promoting subaerial aggradation rather than erosion (Fielding et al., 2003; Johnson et al., 1982; Woolfe et al., 1998). With the exception of a few larger rivers (Fielding et al., 2005; Ryan, Bostock, et al., 2007), carbonate platforms are thought to obstruct most rivers and streams from reaching the shelf edge, causing fluvial sediments to become trapped on the shelf (Dunbar & Dickens, 2003b; Feary et al., 1993; Fielding et al., 2003; Page & Dickens, 2005; Ryan, Bostock, et al., 2007; Symonds et al., 1983; Woolfe et al., 1998). On the continental slope, numerous canyons show signs of presently active or recent (<80 ka) incision (Feary et al., 1993; Puga-Bernabéu et al., 2013; Webster et al., 2012). By re-routing and blocking sediments, the platforms may play a role in preventing the burial of these canyons. However, it is still less clear as to why the canyons remain recently active, particularly as the platforms appear to isolate the canyons from lowstand fluvial sources, which are widely believed to instigate incision within canyon heads (Baztan et al., 2005; Daly, 1936; Kolla & Macurda, 1988; Pratson et al., 2007; Rasmussen, 1994). In the surrounding basin, lowstand submarine fans have not been documented. Instead, flows are characterized by multiple generations of far-reaching sediment gravity deposits and turbidites, which are deposited at all sea level stages (Puga-Bernabéu et al., 2014; Watts et al., 1993). Gaps between the platforms (or “inter-reef passages” at highstand), are believed to act as conduits for deposition of coarse-grained sediments on the slope and in the basin (Puga-Bernabéu et al., 2014; Symonds et al., 1983; Webster et al., 2012).

Sediment cores and seismic data provide clues as to how the margin behaved before the platforms became established on the shelf, potentially lending insight into the more recent impact of platform topography on the margin. Echoing typical siliciclastic systems, deposition of coarse-grained material was high on the slope during lowstands, where it was hypothesized that these sediments could more directly migrate to base level (Feary et al., 1993; Feary & Jarrard, 1993). Additionally, the slope was dominated by broader paleovalleys instead of smaller canyons (Feary et al., 1993; Symonds et al., 1983). These authors note a fundamental shift in margin sedimentation style once the platforms appear in seismic sequences.

This deviation from convention poses challenges when attempting to identify the governing mechanisms that form certain geomorphological features. Process-based models help address these shortcomings by simulating these mechanisms in a numerical framework (e.g., Salles, Ding, Webster, et al., 2018). When simulations reproduce observations, they provide crucial insights into governing physical processes that otherwise may be impossible to observe or ascertain from the geological record alone. As all numerical models are simplified representations of reality, mismatches between observations and simulations are inevitable. However, these mismatches can also be used to identify potentially influential processes that are less understood.

This study aims to test the role of carbonate platforms in reproducing key geomorphological features that have previously been described on the Great Barrier Reef margin. Beginning during the previous lowstand (~30 ka), we run simulations with both a “pre-Holocene” and a “platforms absent” topographic surface, comparing model outputs to multibeam data, seismic sections, backscatter imagery, and interpretations from sediment cores. We show that the platforms play a crucial role in modulating key bedload processes, thus facilitating the formation of outer-shelf paleochannels, inner to mid-shelf fluvial mounds, shelf-edge deltas, slope-confined canyons, and surface gravity flows.

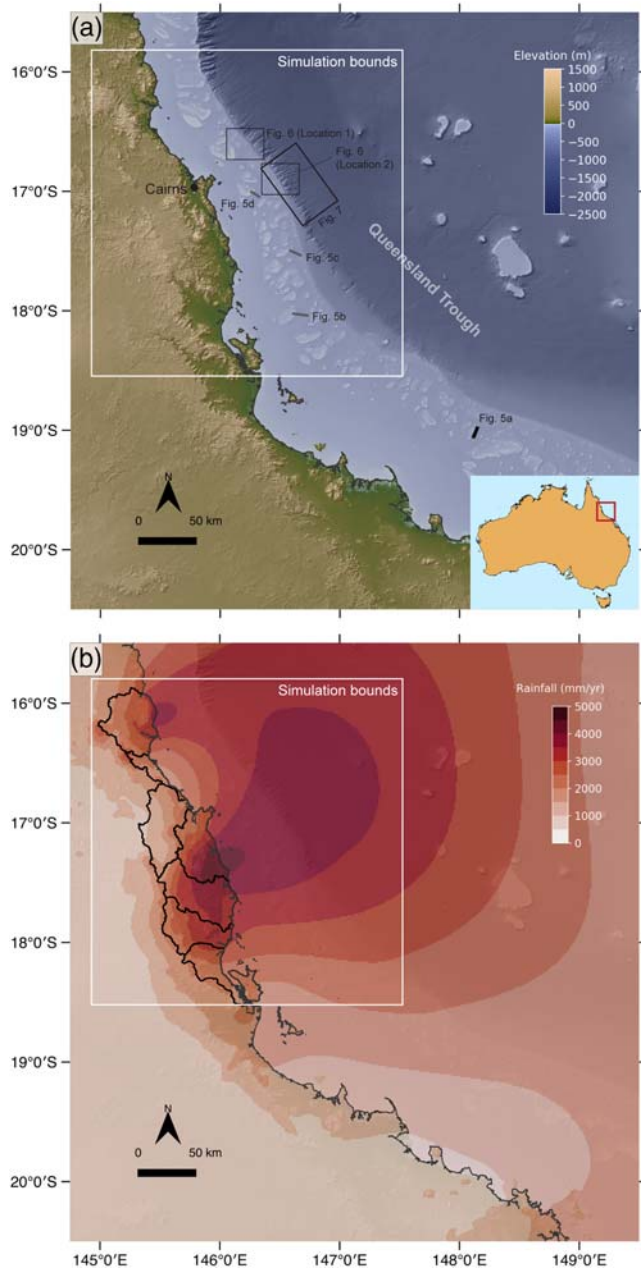


Figure 1. (a) Hillshaded digital elevation model (DEM; Beaman, 2010) of the Noggin region contained within the simulation bounds. Note the positions of the carbonate platforms in pale blue. Figure 5a (black line) denotes an observed seismic location adapted from Johnson and Searle (1984). Figures 5b–5d (gray lines) denote the locations of simulated seismic profiles. Figures 6 and 7 delineate the bounds of close-up renderings of 30 m resolution multibeam data (Webster et al., 2008). They also delineate the corresponding modeled areas shown in Figures 6 and 7. (b) Thirty-year average annual rainfall (Australian Bureau of Meteorology, 2019) with catchments outlined in black (Department of Natural Resources and Mines, 2009).

2. Regional Setting

The study region is located in an area previously referred to as the “Noggin” region (Bridge et al., 2011) on Australia’s central Great Barrier Reef margin near the Queensland town of Cairns (Figure 1a). Now a passive margin, the region’s more active history of extensional tectonics, long-term subsidence, fault reactivation, and tilting gave rise to the large-scale bathymetric geometries that physiographically define the margin today (Davies et al., 1989; Symonds et al., 1983). The margin is characterized by a relatively narrow (~50–80 km) continental shelf, a relatively steep (4–7°) continental slope, and a deep (1,500–1,800 m), north-westward-dipping Queensland Trough (Puga-Bernabéu et al., 2013). Tropical climatic conditions favor coral reef growth on the continental shelf, which facilitated the construction of many large (50–200 km²) carbonate platforms over multiple sea level cycles since the modern Great Barrier Reef’s inception. Proposed ages for the Great Barrier Reef’s initiation range from 400 to 670 ka (Braithwaite et al., 2004; Dubois et al., 2008; Gallagher et al., 2014; International Consortium for Great Barrier Reef Drilling, 2001). This age range is broad, which in part reflects the indirect and imprecise methods so far applied to dating the reef’s initiation. However, this broad range may also represent the interplay of multiple paleoenvironmental factors (i.e., the onset of high-amplitude sea level fluctuations during the mid-Pleistocene, paleoceanographic and paleoclimatic changes) that may have caused the reef’s initiation to occur at different times and at different latitudes (Dubois et al., 2008; Gallagher et al., 2014). The entire Great Barrier Reef margin is classified as mixed carbonate-siliciclastic due to substantial contributions from outer neritic and high-energy reef sources, which supplement typical hemipelagic sedimentation (Davies & McKenzie, 1993; Mount, 1984).

Presently, the Noggin region resides within intermingling wet and dry tropical zones, which are dictated by monsoonal, orographic rainfall (Australian Bureau of Meteorology, 2001). The region is often subjected to monsoon-related flooding and cyclone activity (Sumner & Bonell, 1986), further driving up average annual rainfall values (Figure 1b). As a result of the variable rainfall regime and the topographic control imposed by the mountains to the west, modern rivers and their catchments are comparatively small (~500–2,000 km²), seasonal in flow, and sometimes ephemeral, emptying their sediments in the nearshore (<20 m depth; Neil et al., 2002; Orpin et al., 2004). The region is macrotidal (Ryan, Brooke, et al., 2007), and offshore wave regime is moderately energetic, where both swell and locally generated waves are driven by east-south-easterly winds and power north-westward longshore currents (Gallop et al., 2014; Larcombe et al., 1995; Orpin et al., 2004).

3. Methods

3.1. Overview

In this study, we simulate the geomorphological evolution of the Great Barrier Reef margin using pyBadlands (Salles, Ding, Webster, et al., 2018), a code designed to deterministically model sediment transport and landscape evolution on long (millennial to tectonic) timescales. By capturing

fluvial processes, turbidity currents, carbonate platform accretion, and wave-driven longshore currents, the code is ideally suited to simulating the principal bedload processes that operate on mixed carbonate-siliciclastic, high-energy margins.

We note here that while there are many intriguing questions surrounding the behavior of suspended sediments on this margin (see Dunbar et al., 2000; Page et al., 2003), our code does not account for the entrainment and subsequent dispersal of fine-grained sediments. We instead focus on features that are more likely to be controlled by bedload processes which mobilize coarse-grained material (i.e., fine sand and larger).

The following methods describe the various governing equations, inputs, and boundary conditions implemented in pyBadlands (see Table S1 in the supporting information for a full list of model parameters).

3.2. Clastic Sedimentation and Landscape Evolution

3.2.1. Bedload Fluvial Incision and Deposition

On a first-order basis, fluvial incision occurs on steep slopes that are subjected to high discharge (Tucker et al., 2001). In pyBadlands, this process is simulated using a detachment-limited stream power law (Howard, 1980; Salles & Hardiman, 2016; Tucker et al., 2001):

$$\dot{\epsilon} = -\kappa_e A^m S^n, \quad (1)$$

where $\dot{\epsilon}$ is the vertical incision rate of a river into its bed, κ_e is an erodibility coefficient, A is the drainage area (a proxy for discharge, and it is a function of precipitation), S is the local topographic gradient, and m and n are dimensionless coefficients. The vertical incision rates computed by the stream power law are then used to calculate bedload sediment volumetric fluxes between nodes, which are then tracked throughout the computational domain over time. When simulated rivers or streams encounter shallow local topographic slopes (i.e., $S < 0.3^\circ$ in our experiments), deposition is assumed to occur. Deposition is also permitted in local topographic depressions using a pit-filling algorithm (Planchon & Darboux, 2002).

While the parameters drainage area A and topographic gradient S are iteratively computed from the initial topographic surface (see section 3.6.1), the other parameters are predetermined. The coefficients m and n default to values of 0.5 and 1, respectively (Salles, Ding, Webster, et al., 2018). The erodibility coefficient κ_e depends on a variety of factors that control the detachability of the rock substrate, such as climate, rock strength, vegetation, and channel hydraulics (Lague et al., 2005; Whipple & Tucker, 1999). As these factors are not easily quantifiable, and because the parameter is scale-dependent (Dietrich et al., 1995), the onshore bedrock erodibility coefficient is calibrated by directly comparing the computed sediment fluxes in the model to observed sediment fluxes in the field. The coefficient is then altered until the computed and observed fluxes match to the correct order of magnitude. Belperio (1979) determined that riverine sediment in the central Great Barrier Reef region is composed of approximately 10–20% bedload. Using this ratio, we calibrated κ_e to a value of $9.0 \cdot 10^{-8}$ using total annual sediment load estimates from the Tully River mouth (Brodie et al., 2009). This river has undergone long-term monitoring and lies within the computational domain, allowing for region-specific calibration of subaerial bedrock erodibility. We assign a separate κ_e value for the shelf, slope, and basin, where we assume that sediments are more detachable in these settings. We set κ_e to a value of $7.5 \cdot 10^{-6}$ on the basis that key erosional morphological features (e.g., submarine canyons and outer shelf paleochannels) are reproduced. The selection procedure for shelf, slope, and basin erodibility is necessarily qualitative given that the observed sediment fluxes required for site-specific calibration are unavailable for these areas.

The code solves the continuity equation using a finite volume scheme on an irregular triangulated mesh of approximately 250-m resolution (Tucker et al., 2001). Flow is assumed to occur unidirectionally along the slope of steepest descent (O'Callaghan & Mark, 1984). To ensure numerical stability and adequate temporal resolution, an adaptive time step is implemented (Salles & Hardiman, 2016), where the maximum time step interval is set to 100 years.

3.2.2. Turbidity Currents and Marine Sedimentation

In pyBadlands, the stream power law (equation 1) is also used to approximate long-term submarine erosion and deposition by turbidity currents and surface gravity deposits. In this case, the onshore fluvial network is extended below mean sea level and also operates as a submarine hyperpycnal flow network. For the hyperpycnal flow network, parameters A and S in the stream power law are modified, following Petit et al. (2015). Drainage area A remains confined to onshore catchment rather than appending the additional area gained by the hyperpycnal flow network, and an effective slope is computed to reduce the erosive power of rivers and streams when they meet the ocean. Thus, erosion rate $\dot{\epsilon}$ is dependent on S_{eff} :

$$S_{eff} = S \frac{\rho_{sed} - \rho_{wat}}{\rho_{sed}}, \quad (2)$$

where ρ_{sed} is the sediment density and ρ_{wat} is the water density.

In the model, submarine erosion by turbidity currents is simulated when sediments chronically oversaturate the hyperpycnal flow network over long periods of time. When the critical density of the combined water and sediments surpass a given threshold (1,000.025 kg/m³; see Table S1), erosion and downcutting occurs, and sediments are entrained within the hyperpycnal flow network. This threshold value is necessarily low because the timescale of the model does not permit turbidity currents to be triggered instantaneously and episodically. Here, the erosive action of turbidity currents is simulated over longer timescales. As a result, the density threshold value needed to trigger long-term erosive action by turbidity currents must be lowered.

To avoid frequent and rapid avulsion, and to enable sediments to be distributed downslope, the proportion of sediments deposited at a particular cell, d_{prop} , is a function of the local slope:

$$d_{prop} = \frac{0.9}{1 + e^{\alpha(S-0.005)}}, \quad (3)$$

where α is a scaling parameter. Sediments therefore are permitted to bypass steeper slopes and are deposited on shallower slopes (Lowe, 1976).

3.2.3. Creep and Slope Failures

In pyBadlands, soil creep is modeled using a well-known linear diffusion law (Braun et al., 2001; Sweeney et al., 2015):

$$\frac{\partial z}{\partial t} = \kappa_d \nabla^2 z, \quad (4)$$

where z denotes topographic elevation and κ_d is a diffusion coefficient with units of L²/t. Saunders and Young (1983) determined a value of $\kappa_d \approx 0.0008$ m²/year for tropical climates, which falls within the accepted order of magnitude for creep rates on land (Martin & Church, 1997). In the deep marine realm (i.e., below wave base), creep diffusion is less efficient (Jordan & Flemings, 1991; Schlager & Adams, 2001), and thus a lower value of $\kappa_d = 0.0001$ m²/year is prescribed based on observations from Maryland coastal plains (Carson & Kirkby, 1972; Fagherazzi et al., 2004).

Downward movements due to instantaneous slope failure are similarly approximated by the linear diffusion law. When local topographic slope exceeds a critical threshold ($S > 14^\circ$), a higher κ_d value (0.2 m²/year) is assigned, resulting in accelerated diffusion on steep slopes. This κ_d value is informed by measured landslide transport rates (Martin & Church, 1997).

3.3. Waves and Longshore Drift

Where energy conditions permit, wave action propels longshore drift in the nearshore environment. Here, we parameterize the long-term sedimentary impact of longshore drift using a linear, shallow water wave formulation. The basic procedure is as follows: using initial wave forcing parameters (see section 3.6), wave transformation is computed in the domain, where the algorithm accounts for energy dissipation due to breaking and bottom friction (Salles, Ding, Webster, et al., 2018). Once a critical shear stress threshold is surpassed at bed, sediments are entrained and transferred parallel to the isobath beneath the breaking zone. Upon entering an area where the bottom shear stress falls below the threshold value or where the depth falls below the prescribed maximum wave base, sediments are once again deposited. Here, the maximum wave base is set to 20 m based on wave data collected near the study region (Orpin et al., 2004). For a full breakdown of the governing equations for wave transformation and longshore drift, see Salles, Ding, and Brocard (2018).

3.4. Carbonate Platform Accretion by Coral Reefs

The vertical accretion of carbonate platforms by coral reef ecosystems is simulated using the fuzzy logic approach of Salles, Ding, and Brocard (2018). The approach involves the application of a set of user-defined conceptual rules that dictate whether reef growth occurs. Three critical, first-order factors control accretion rates on geological timescales: water depth (which modulates light exposure and accommodation space), wave activity, and clastic sedimentation rate. When these conditions are simulated in

pyBadlands (Salles, Ding, Webster, et al., 2018), reef growth will either be permitted or limited on carbonate platforms via an if-then logic. For instance, if carbonate platforms lie within a particular water depth range, then they will undergo vertical accretion by corals and other calcifying organisms. Conversely, if the platforms are subaerially exposed, then reef growth will not occur, and carbonate platforms will not undergo vertical accretion. In the model domain, reef growth is permitted on carbonate platforms, as it is generally accepted that a hard, antecedent Pleistocene substrate provides the necessary structural foundations for subsequent Holocene and modern reef growth (Davies & Marshall, 1980; Hopley et al., 2007; Johnson & Searle, 1984; Marshall & Davies, 1982).

Following Salles, Ding, and Brocard (2018), the conceptual framework set by these rules is then translated into a quantitative framework in the numerical model. The controlling factors of coral reef growth (i.e., depth, wave height, and clastic sedimentation rate) are represented by a series of membership functions (see Figure 7 in Salles, Ding, & Brocard, 2018), where we consider a unique set of functions for both a shallow and a deep species assemblage. For each environmental factor, the degree of fuzzy membership peaks over a specified range, thus providing a window that allows for optimal growth. The degree of fuzzy membership yielded by these functions is then mapped to a physical carbonate accretion rate according to a maximum real-world value (Zadeh, 1965). Maximum accretion rates were informed by core-derived rates for shallow facies (i.e., robust branching corals; 1.2 cm/year) and deep water facies (i.e., tabular-branching and massive corals; 1.0 cm/year; see Montaggioni, 2005) from reefs in the Indo-Pacific.

3.5. Pelagic Sedimentation

In addition to coral reefs, pelagic organisms contribute to carbonate deposition on the northeastern Australian margin. This process is simulated through a similar fuzzy logic method, where the sedimentation rate is only dependent on depth. An upper limit of 1.0 cm/kyr was prescribed based on sedimentation rates computed from basin piston cores containing over 90% carbonate (Dunbar et al., 2000). We assume that the effects of compaction are negligible over the past 30 kyr.

3.6. Initial and Boundary Conditions

3.6.1. Bathymetry and Topography

To test the impact of the carbonate platforms on the geomorphological development of features on the margin, we constructed two topographic surfaces: a “pre-Holocene” surface and a “platforms absent” surface. First, to construct a pre-Holocene surface, we assume the most significant and consequential changes in elevation and shelf gradient occurred due to transgressive and highstand carbonate accretion on carbonate platforms. Though variable, Holocene reef thicknesses generally peak at ~15 m (Marshall & Davies, 1984; Webster & Davies, 2003). Following Salles, Ding, Webster, et al. (2018), the initial topographic surface was extracted and smoothed from a 100 m resolution DEM spanning the entire Great Barrier Reef margin (Figure 2a; Beaman, 2010). We then remove a layer with a maximum thickness of 15 m at shallower platform depths, tapering the layer linearly at deeper platform depths (Figure 2b) to produce the final pre-Holocene surface (Figure 2c). Finally, to construct the “platforms absent” surface, we excised all carbonate platforms and applied a linear interpolation over removed shelf areas (Figure 2d). While this surface is artificial, we aimed to preserve the general underlying geometry of the margin for direct comparison, thereby isolating the impact of the platforms. We assume the effects of tectonic subsidence are negligible (Webster et al., 2018), and we assume that onshore river catchments have not significantly reorganized during the last 30 kyr based on pollen records from ODP Site 820 (Moss & Kershaw, 2007).

3.6.2. Sea Level

To simulate sea level rise and fall, we use the curve of Grant et al. (2014). We opted for a curve which approximates global eustatic sea level rather than a locally derived one because the millennial-scale factors that modulate local accommodation space (e.g., fluvial supply and marine deposition; Posamentier et al., 1988) are independently simulated in the model. Similarly, for this study we chose not to use sea level curves reconstructed solely from coral reef proxies (i.e., Yokoyama et al., 2018—IODP Exp. 325 from the Great Barrier Reef) to prevent a self-confirming result in the carbonate accretion module.

3.6.3. Precipitation

As fluvial sedimentation relies on precipitation, we force the model using an average annual rainfall data set spanning 30 years (Figure 1b; Australian Bureau of Meteorology, 2019), which captures critical orographic rainfall patterns. Though regional pollen proxies suggest millennial-scale rainfall variability (Burrows

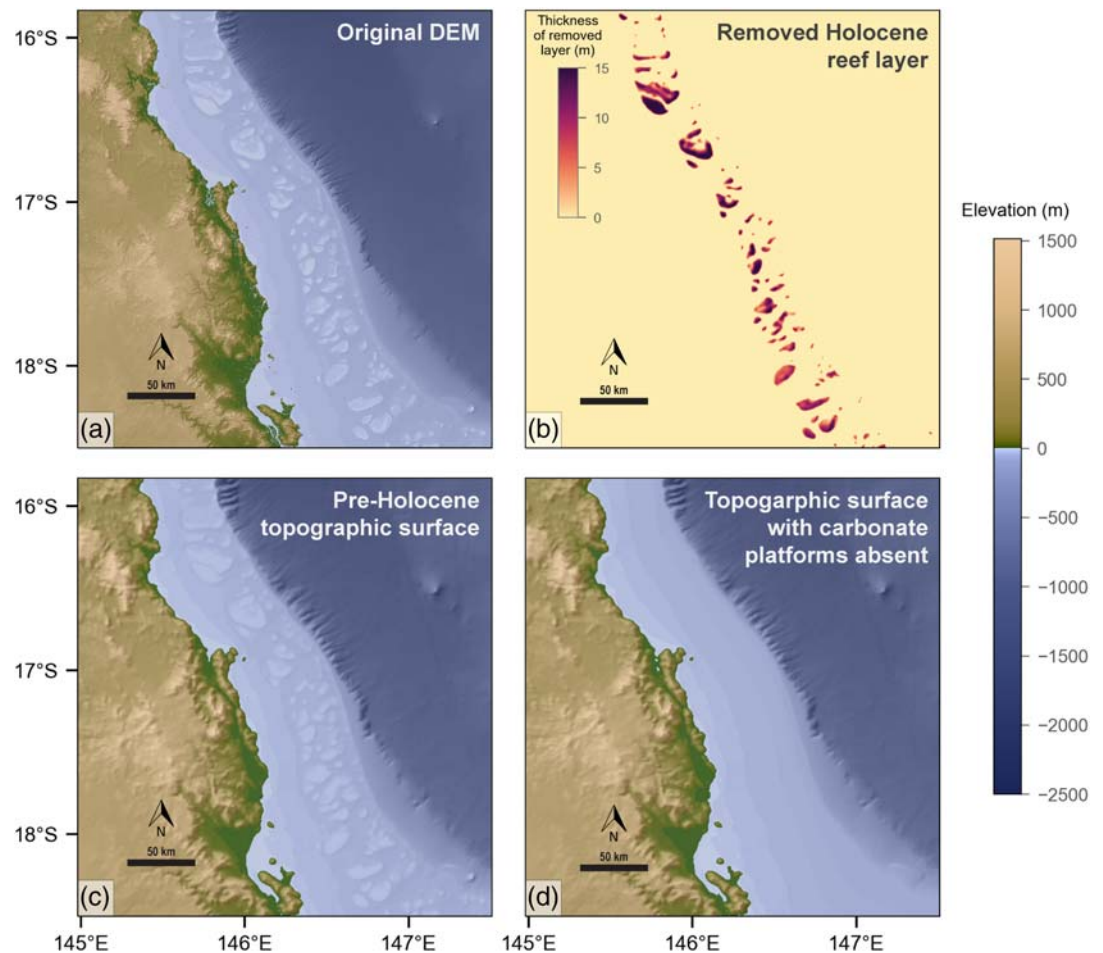


Figure 2. (a) Original DEM spanning the computational domain. (b) Thickness representing the most recent Holocene reef growth on platforms. This layer was removed from the original DEM to produce the pre-Holocene surface depicted in the next panel. (c) Smoothed pre-Holocene topographic surface. (d) Artificial surface with carbonate platforms removed entirely.

et al., 2016; Hughes & Croke, 2017), specific rainfall values are often difficult to precisely reconstruct, complicating the model forcing. In light of the uncertainty inherent in reconstructing paleoclimate parameters, we retain this precipitation regime over the duration of the model to highlight the influence of other environmental variables we are most interested in testing (i.e., the impact of the carbonate platforms).

3.6.4. Wave Regime

Based on output from a global hindcast model, which centers on the wind wave climate of Australia and the South Pacific (Durrant et al., 2014), we prescribe an easterly wave direction and a significant wave height of 2.0 m as boundary conditions for the wave module. The hindcast model predictions are in good agreement with measured wave heights from satellite altimetry (Gallop et al., 2014). While the late Pleistocene and Holocene wave climate for central Queensland is still poorly understood, major climatic phenomena such as El Niño–Southern Oscillation (ENSO) have likely experienced variability over this time (Shulmeister & Lees, 1995). The wave climate of the southwest Pacific, being tightly coupled to ENSO (Goodwin, 2005), may have responded to these changes. Nonetheless, we retain these wave parameters over the course of the simulation for simplicity.

4. Results

4.1. Regional Outlook

Before focusing on specific geomorphological features, we provide a regional overview of river, shoreline, and carbonate platform evolution to help visualize the development of the Noggin margin as it progresses

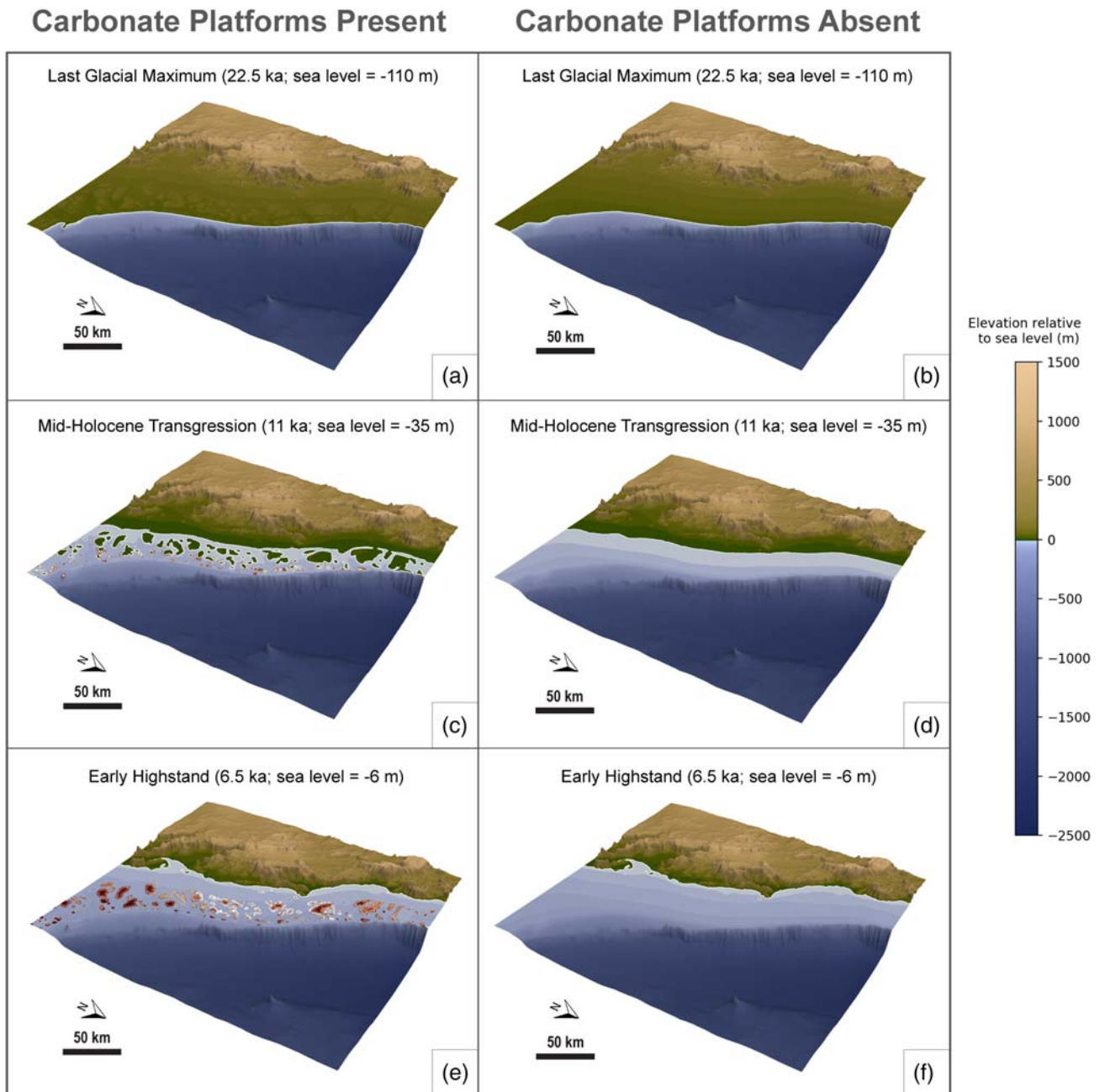


Figure 3. Three-dimensional rendering of model output depicting the migration of the shoreline at key times: the Last Glacial Maximum (22.5 ka), the mid-Holocene transgression (11 ka), and the beginning of the Holocene highstand (6.5 ka). The first column illustrates the shoreline position in the simulation where carbonate platforms are present in the initial topographic surface, and the second column illustrates the shoreline position in the simulation where carbonate platforms are absent. Orange indicates areas where shallow and deep coral reef assemblage growth has become activated in the simulation. This occurs when water depth, wave conditions, and sedimentation rates are suitable (see section 3.4). Vertical exaggeration = 11 \times .

through lowstand (30–15 ka), transgression (15–6.5 ka), and highstand (6.5 ka–present). We highlight notable differences in the regional evolution of the margin when platforms are present and when platforms are absent.

Model outputs showcase differences in nearshore geometry at key times (Figure 3). During the Last Glacial Maximum (22.5 ka, sea level = -110 m; Grant et al., 2014), relict platform geometries manifest as subaerially exposed karstified hills, with the shoreline rimming the outer shelf break (Figure 3a). Karstified hills are

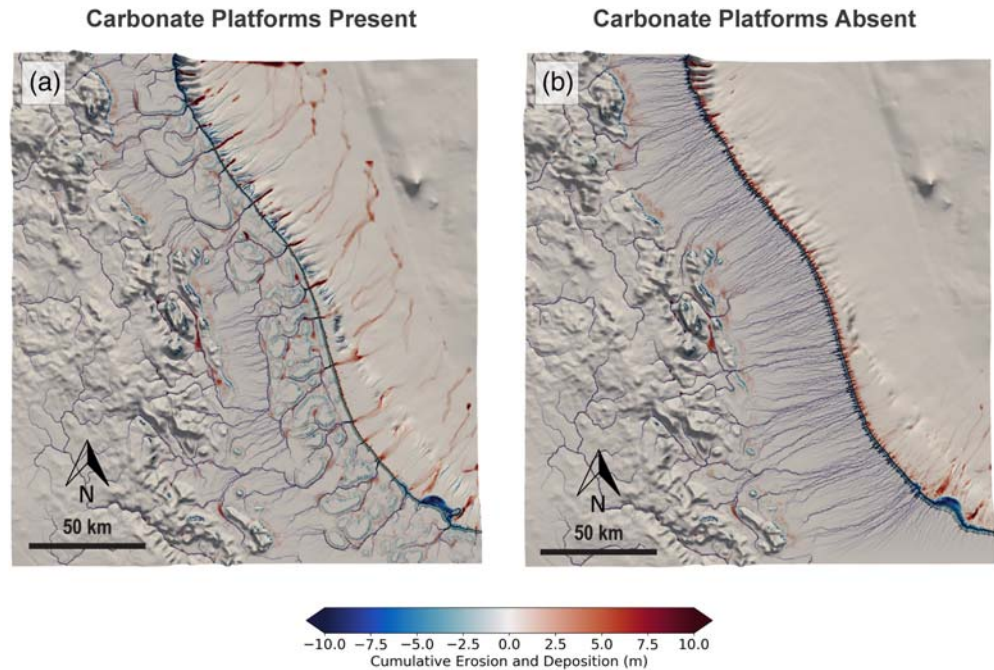


Figure 4. Drainage network evolution from lowstand (30 ka) to the beginning of the transgression (15 ka) for simulations containing carbonate platform topography (a) and no carbonate platforms (b). Major rivers and streams computed in the model are shown in blue, where drainage patterns at 30, 25, 20, and 15 ka are overlain over cumulative erosion and deposition over this period. Red areas around the carbonate platforms indicate deposition of both platform and fluvial sediments.

absent from the “platforms absent” simulation by design, and the shoreline occupies a similar shelf-break location due to the preservation of upper slope geometry in constructing the initial artificial surface (Figure 3b). During the mid-transgression (11 ka, sea level = -35 m) shoreline geometries diverge considerably. When platforms are present, the paleoshoreline advances landward (Figure 3c) but is punctuated by subaerially exposed karstified hills, forming a series of topographically complex coastal embayments that fall within wave base. Contemporaneously on the outer shelf, smaller submerged platforms begin to undergo vertical accretion by shallow and deep coral assemblages. Prolific reef growth atop platforms begins at ~ 9 ka when they become fully flooded. This is largely consistent with turn-on times indicated by fossil reef cores recovered on the shelf edge (Webster et al., 2018) and inner to mid-shelf (Hopley et al., 2007). When carbonate platforms are absent, the shoreline is more uniform and linear during the transgression (Figure 3d), owing to the more gradual underlying shelf gradient. Finally, during the highstand “carbonate platforms present” scenario (6.5 ka, sea level = -6 m), the shoreline reaches a similar position to that of present day (Figure 3e), and reef growth continues. The “platforms absent” scenario attains a similar shoreline configuration but without the proliferation of reefs (Figure 3f).

Lowstand fluvial networks are profoundly reorganized by the presence of the platforms, where rivers and streams are often re-routed and coalesce within gaps between platforms on the outer shelf (Figure 4). Localized sediment mounds are constructed around the platforms by a combination of re-deposited fluvial and platform-derived sediments. These re-routed rivers produce outer-shelf paleochannels, shelf-edge deltas, and highly localized slope and basin flows, all of which will be discussed in greater detail in the following results sections. When carbonate platforms are removed, rivers and streams follow a more direct route to the outer shelf, primarily depositing their sediments on the outer shelf and upper slope. Particularly notable is a lack of incision on the inner to mid-shelf in both cases.

4.2. Shelf Features

Model simulations reproduce notable shelf features observed in seismic data, including reef pinnacles, reworked transgressive shelf deposits, fluvial mounds, shelf-edge paleochannels, and shelf-edge deltas. These features do not appear in the same fashion when carbonate platforms are removed.

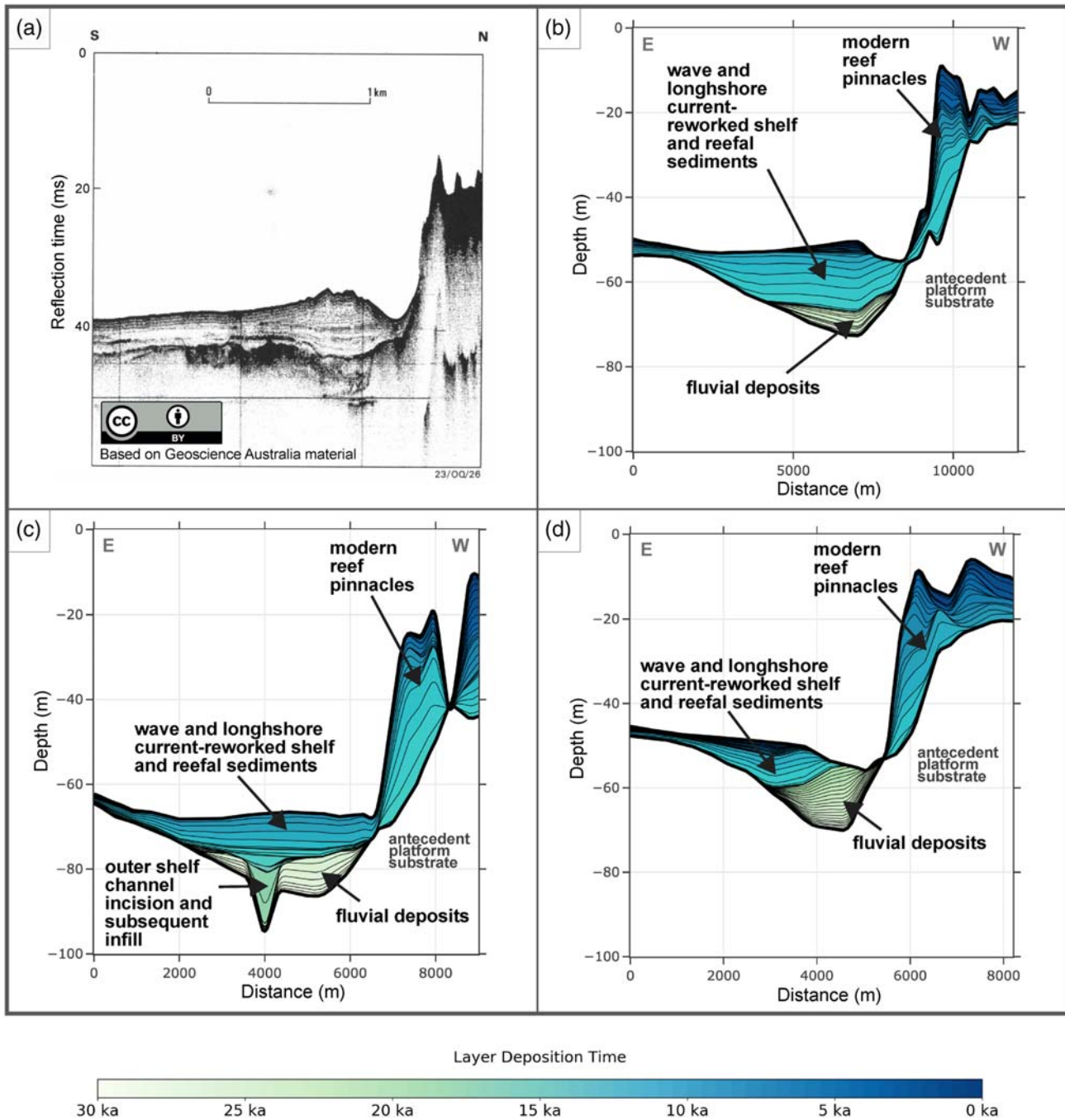


Figure 5. (a) Boomer profile showing sediment mounds overlying a channel on the windward margin of Prawn Reef (adapted from Symonds et al., 1983). (b–d) Examples of synthetic seismic cross sections showing positive relief and mounding over bathymetric depressions rimming the windward margins of various carbonate platforms in the computational domain. For locations of all lines, see Figure 1.

Starting on the mid-shelf, it is important to note that the observed seismic cross-section fell outside of the simulation bounds, precluding direct data-model comparisons at this specific site. Here, we opted to provide several simulated examples from multiple locations within the domain. The observed seismic section along the windward edge of Prawn Reef illustrates mounded morphology at the base of a reef pinnacle (Figure 5a), where vibrocores from the mound recovered fluvially-derived sands (Symonds et al., 1983). Simulations produce similar mounded morphologies at the bases of modern pinnacles, where mounds are partially constructed by Pleistocene fluvial deposits and reef talus at lowstand. They are further shaped by reworked

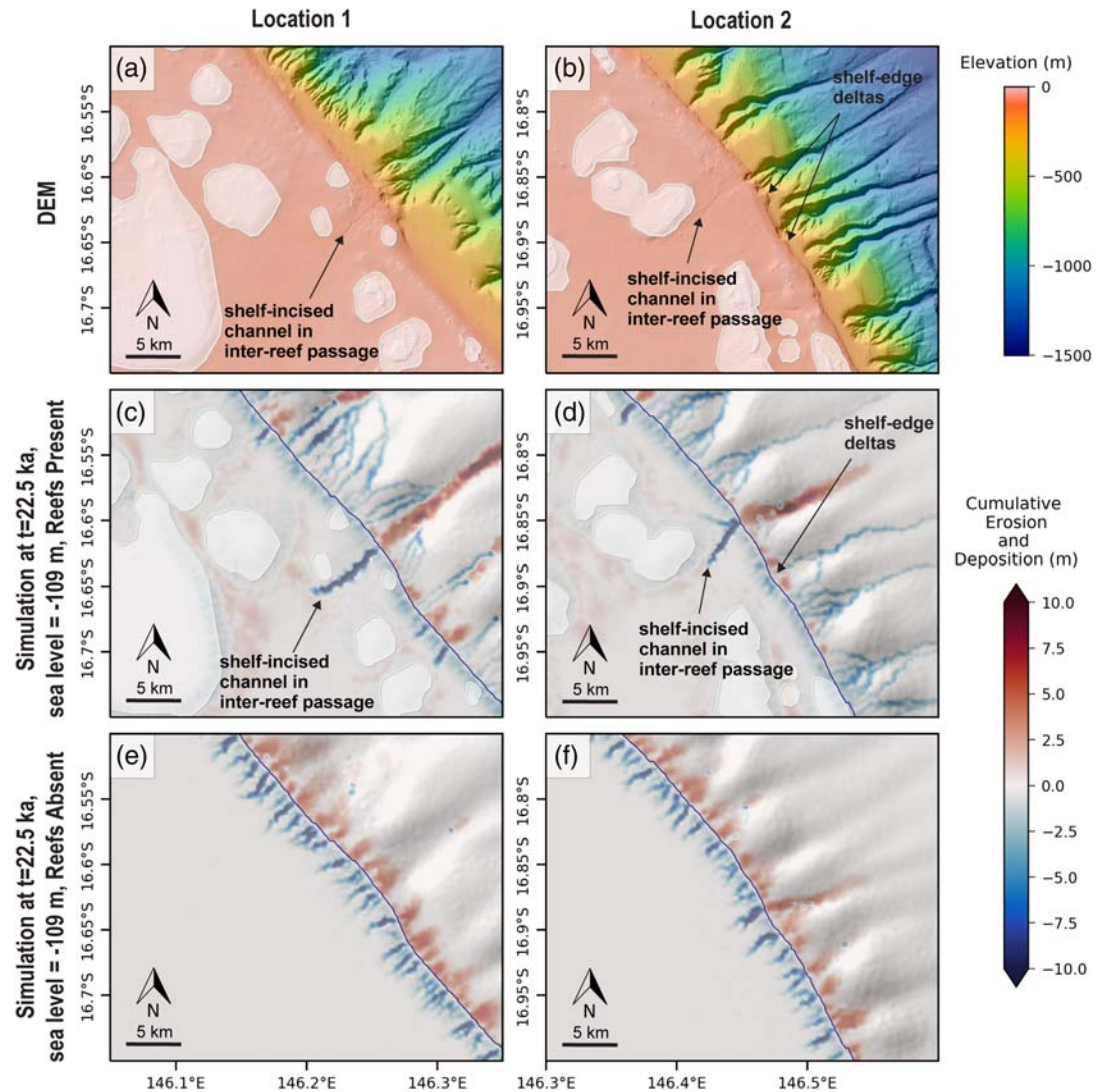


Figure 6. Feature comparison of DEM and simulated cumulative deposition/erosion (temporal range: 30–22.5 ka) for two outer-shelf locations. The blue lines indicate sea level position, and carbonate platforms are shaded in white. For locations, see Figure 1.

shelf and platform-derived sediments during the transgression (Figures 5b–5d). A lowstand erosional channel was also incised in the model (Figure 5c), where it was subsequently backfilled by channel abandonment, waves, and currents during the beginning of the transgression. In simulations, carbonate vertical accretion commences around the antecedent platform edge at ~14 ka. Upward growth propagates across the top of the platform after it becomes fully inundated at ~9 ka.

Outer shelf features that were reproduced in model simulations include paleochannels (sometimes referred to as “shelf-incising canyons”) and shelf-edge deltas (Figure 6). Paleochannels are excavated via knickpoint retreat by lowstand rivers, which regain stream power when they are directed through gaps between platforms. When carbonate platforms are removed, minor shelf-edge incision occurs, but paleochannels are much shorter and are uniform along the shelf-edge. Similarly, shelf-edge deltas appear in both simulations, but their occurrence is more scattered when carbonate platforms are present.

4.3. Slope Features

The highly gullied, dendritic morphologies of the Noggin region canyons were successfully reproduced in model simulations when carbonate platforms were present (Figures 7a and 7b). Also reproduced are

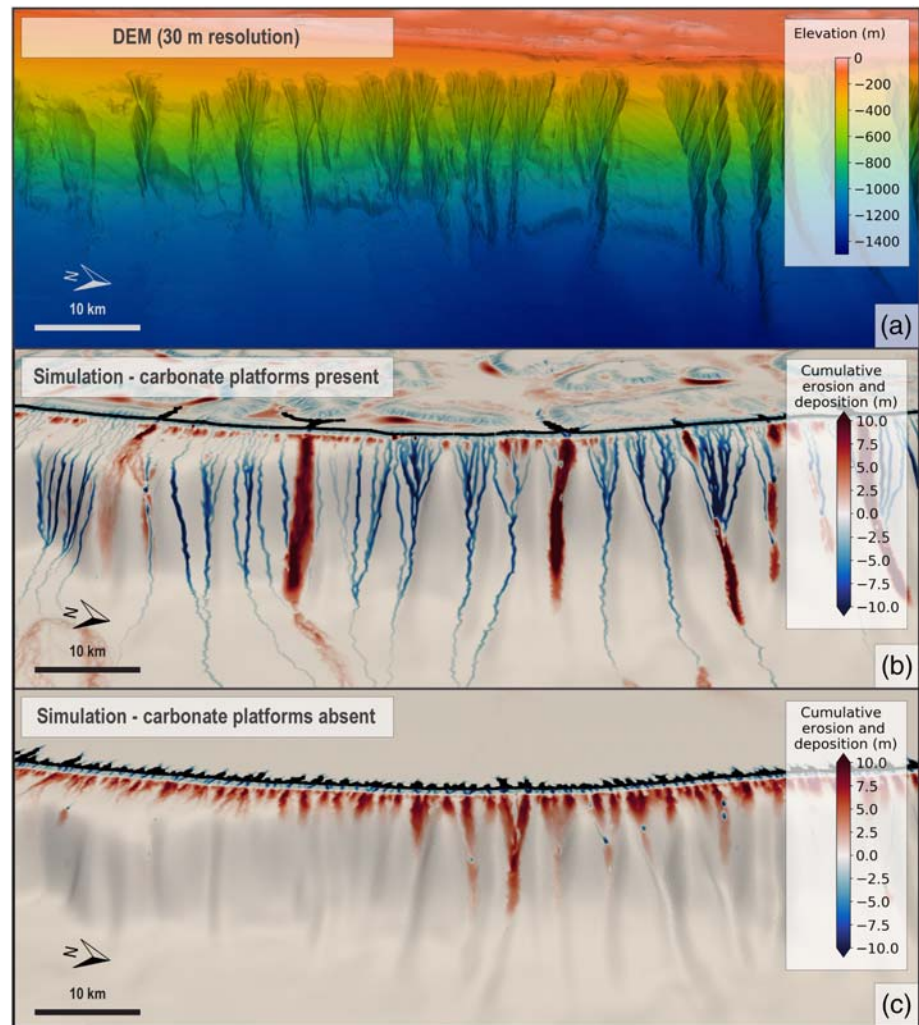


Figure 7. (a) High-resolution (30 m) multibeam bathymetry showing dendritic canyon morphologies described in the Noggin region (Puga-Bernabéu et al., 2013). (b) Simulations of cumulative erosion and deposition in the Noggin region from 30 to 15 ka (i.e., lowstand to early transgression), where carbonate platforms are present and dendritic morphologies of the canyons are reproduced by turbidity current incision. (c) Identical simulation of the Noggin region with carbonate platforms absent. Vertical exaggeration = 11X.

linear, more isolated gullies to the south. In the model, incision is instigated throughout the lowstand by the triggering of erosive turbidity currents, where turbidity currents are initiated by an excess of sediments eroded from steep platform, shelf edge, and upper slope topography. The smoothed, antecedent slope topography also controls gully orientation, where individual channels in the amphitheater heads coalesce further downslope. Canyon head incision is interspersed with shelf-edge and upper slope fluvial deposits. When carbonate platforms are removed from the simulation, canyon incision by this process ceases entirely (Figure 7c). Instead, the outer shelf edge and upper slope experience more uniform net deposition during this lowstand period.

4.4. Basin Features

Backscatter data depict surface gravity deposits on the slope and in the basin in the Noggin region, where two major northward-deflecting flows have previously been interpreted (Figure 8a; Dunbar et al., 2000). Corresponding simulations with carbonate platforms produce a variety of northward-deflected gravity deposits during lowstand (Figure 8b), which are facilitated both by erosive turbidity currents and by highly localized deposition on the slope in gaps between platforms. In the model, flows extend into the axis of the

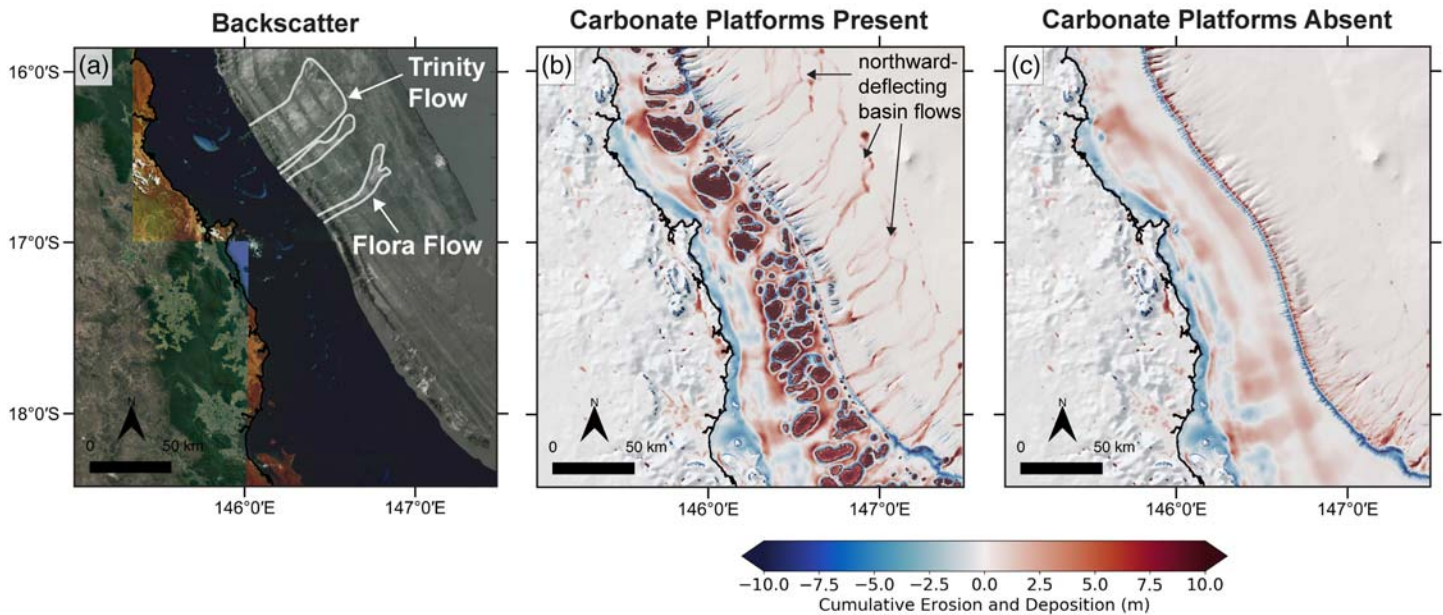


Figure 8. (a) GLORIA side-scan sonar backscatter imagery (Puga-Bernabéu et al., 2013), pictured with satellite imagery of the onshore and shelf areas. White areas on the slope and in the basin correspond to areas of high reflectivity, interpreted as coarse-grained surface gravity deposits and landslides. Labeled flow names follow the interpretations of (Dunbar et al., 2000). (b) pyBadlands simulation output with carbonate platforms present, depicting shelf-to-basin cumulative erosion and deposition from 30 to present. (c) Cumulative erosion and deposition for the “platforms absent” simulation.

Queensland Trough and appear to be fairly evenly distributed from north to south. When carbonate platforms are absent (Figure 8c), turbidity currents are not readily triggered, with deposits more concentrated on the upper slope. Another notable feature is the lack of submarine fans in both cases.

5. Discussion

A number of geomorphological features are successfully reproduced with pyBadlands when carbonate platforms are present in the initial topographic surface. Within each Discussion section, we will investigate the mechanisms that are responsible for forming them in the model space. We reproduce observations in data sets that both pre-date (i.e., seismic reflection profiles and slope/basin sediment cores) and post-date (i.e., seismic reflection profiles, shallow sediment cores, multibeam bathymetry, and backscatter data) the Great Barrier Reef’s inception, lending legitimacy to our approximation of a bathymetric surface without carbonate platforms. This allows us to highlight the role of the reef structure in preconditioning and modifying some of these source-to-sink mechanisms. Additionally, we will discuss areas where the data and model diverge, identifying model limitations and suggesting areas for future work. Table 1 summarizes the model’s ability to reproduce specific features, providing explanations of governing model processes and recommendations for processes that are missing from the model but are potentially important.

5.1. Shelf Features

5.1.1. Sediment Mounding Around Karstified Hills

Our simulations demonstrate that carbonate platforms on the continental shelf obstruct rivers and facilitate mounding of fluvio-deltaic and shelf-derived sediments during lowstand. At a smaller scale, the model is able to reproduce the mounded morphologies of fluvially-derived sands that have been seismically imaged around the windward margins of carbonate platforms (Figures 5b–5d; Symonds et al., 1983). Lowstand mounding is promoted by sharp changes in topography, and subsequent transgressive mounding is instigated by wave-driven longshore drift. However, there are finer-scale discrepancies between observed and modeled morphologies. For instance, observed mounds tend to be smaller, exhibit higher local relief, and are bordered by deeper channels. Such discrepancies suggest that additional, secondary controls (i.e., channel-levee and delta lobe deposition, reworking by wind and tidal currents) may be interacting with

Table 1
Summary of Model's Ability to Reproduce Certain Morphological Features

Feature	Model's ability to reproduce	Processes responsible in model	Potentially missing first-order processes	Key references
Fluvial mounding around platforms	Well-reproduced	Decrease of stream power by steep, subaerially exposed platform topography, local undulations in bathymetry, ample supply from hinterland	Smaller-scale fluviodeltaic processes (delta lobe deposition and channel-levee processes), bottom currents	Symonds et al. (1983), Dunbar et al. (2000), Maxwell and Swinichatt (1970)
Inner shelf paleochannel incision	Poorly reproduced	—	Tidal processes, episodic flooding events	Carter et al. (1993), Fielding et al. (2003; 2005), Johnson et al. (1982), Johnson and Searle (1984), Ryan, Bostock, et al. (2007), Symonds et al. (1983), Orme et al. (1978)
Outer shelf paleochannels	Well-reproduced	Knickpoint retreat driven by subaerially exposed shelf edge, steep upper slope, and increased stream power by rivers and streams, which are re-routed and coalesce within gaps between exposed platforms	Tidal currents	Abbey et al. (2011) and Hinestrosa et al. (2016)
Shelf-edge deltas	Well-reproduced	Knickpoint retreat, relatively low fluvial supply	Two-way coupling of wave-delta interactions	Harris et al. (1990) and Symonds et al. (1983)
Slope-confined canyons	Well-reproduced	Incision by turbidity currents, which are preconditioned by steep carbonate platform topography, steep continental slope, and initial "amphitheater-like" slope morphology	Upslope, retrogressive erosion by landslides and other mass movements	Puga-Bernabéu et al. (2011, 2013)
Sediment gravity flows/turbidites	Partially reproduced	Relatively low supply, relatively steep platforms and continental slope, north-westward deepening geometry of the Queensland Trough	Highstand shedding, river plumes, storm and flooding events, seismicity, and factors influencing slope stability	Dunbar et al. (2000), Puga-Bernabéu et al. (2011, 2014), Watts et al. (1993), Webster et al. (2012)

Note. Also listed are the governing model mechanisms, recommendations for potentially missing mechanisms, and key references.

platforms during and/or following the deposition of the main mound, as has been previously suggested (Symonds et al., 1983).

A regional view of the simulation output shows similar depositional patterns around local topographic highs and within local topographic lows (Figure 4). Once again, small coastal rivers and streams lose their power when encountering the variable relief introduced by the exposed carbonate platforms. This phenomenon has previously been hypothesized to explain the widely reported aggradational shelf geometries observed in seismic sections and the absence of lowstand siliciclastic sediments in slope and basin cores (Dunbar et al., 2000; Dunbar & Dickens, 2003b; Feary et al., 1993; Feary & Jarrard, 1993; Page et al., 2003; Page & Dickens, 2005; Woolfe et al., 1998), representing a significant deviation from conventional reciprocal sequence stratigraphic models (Jervey, 1988; Posamentier et al., 1988; Posamentier & Vail, 1988). However, not all sediments appear to be trapped on the shelf during lowstand; while a portion of both fluvial sediments and reef talus remain on the shelf during this time, our simulations also show highly localized delivery of sediments between carbonate platforms (Figure 4). This behavior has been suggested in previous studies of slope hemipelagic and turbidite sedimentation (Feary et al., 1993; Francis et al., 2007; Puga-Bernabéu et al., 2014). A more detailed source-to-sink computational analysis is warranted to help disentangle the specific sediment sources contributing to these deposits and to determine the fate of these sediments following the transgression. Nevertheless, our model supports the occurrence of both blocking and re-rerouting of sediments that traverse the shelf, processes which do not occur when carbonate platforms are absent (Figure 4).

5.1.2. Paleochannel Incision

Model simulations indicate that outer shelf paleochannel incision is facilitated by the carbonate platforms (Figure 6). In the model, these channels form due to knickpoint retreat, which is prompted by the increased stream power of lowstand rivers as they coalesce through gaps between platforms and flow down the steep shelf edge. When platforms are not present, this process is much less pronounced given the diffuse

distribution of rivers and streams on the outer shelf, which lessens their individual stream power (Figure 6). Because tidal currents are not simulated here, we cannot fully discount their role in forming and maintaining these channels, as has been previously proposed (Abbey et al., 2011; Harris et al., 2005). However, given that the model adequately reproduces these features without tidal activity, we deem platform-facilitated knickpoint retreat to be an important driver in their formation. In reproducing these outer shelf channels, our simulations suggest that lowstand rivers indeed reach the shelf edge because of the lack of a continuous, rimmed barrier in the Noggin region. However, before reaching the shelf edge, they are heavily re-routed and localized through gaps in the platforms, where they then incise the outer shelf. This implies that the positions of these outer paleochannels may not distinctly correspond to the positions of larger onshore rivers and may help explain the sometimes discontinuous nature of shelf-traversing paleochannels in this region (Carter et al., 1993; Fielding et al., 2003). This also implies that paleochannel incision on the outer shelf is instigated by different processes than those on the inner shelf (see below).

Conversely, our models do not reproduce paleochannel incision on the inner and mid-shelf, regardless of whether carbonate platforms are present. This suggests that the shallow and patchy nature of the paleochannels cannot necessarily be attributed to the obstruction of carbonate platforms alone and that other factors may be important. Given their seemingly fragmentary distribution, the origins of the inner to mid-shelf paleochannels, which were imaged roughly 150–200 km southwest of the computational domain (Carter et al., 1993; Fielding et al., 2005; Johnson et al., 1982; Johnson & Searle, 1984; Ryan, Bostock, et al., 2007; Symonds et al., 1983), have been a subject of debate in recent years. Again, while many prominent paleochannels indeed appear to be associated with major rivers (i.e., the Burdekin and Fitzroy; Fielding et al., 2005; Ryan, Bostock, et al., 2007), it has been speculated that many auxiliary rivers and streams in this region would not have been strong enough to incise the low-gradient shelf and that other processes (i.e., tidal scouring and high-energy flooding events) may be contributing to their formation and maintenance during regressions and/or lowstands (Ryan, Bostock, et al., 2007; Woolfe et al., 1998). The modeling presented here supports this view. If inner to mid-shelf paleochannels are indeed present in the Noggin region, we anticipate that stream power would not be high enough to be the sole mechanism responsible for their incision due to small catchment sizes and the shallow shelf gradient. This suggests that other lesser-known incision and maintenance processes might be at play that are not captured in the present model framework. We reiterate the conclusions of Fielding et al. (2005) and Ryan, Bostock, et al. (2007), where paleochannel incision could be quite complex and could involve a number of site-specific factors that preclude formulating a unified model for the region.

5.1.3. Shelf-Edge Delta Formation

Shelf-edge deltas are another byproduct of fluvial deposition and knickpoint retreat in the model (Figure 6). These features also arise when platforms are absent, though they are more uniform along the slope. There is considerable evidence of shelf-edge delta development from seismic reflection data (Symonds et al., 1983) and sediment cores (Harris et al., 1990), where they occur in sequences that both precede and post-date the proposed age range for the inception of the modern Great Barrier Reef (~400–670 ka; Braithwaite et al., 2004; Dubois et al., 2008; Gallagher et al., 2014; International Consortium for Great Barrier Reef Drilling, 2001). The modeling results presented here provide an additional independent line of evidence that favors lowstand shelf-edge delta deposition rather than the development of deep-sea fans, and we attribute this behavior to the relatively low stream power and sediment supply of coastal rivers and streams in the Noggin region. In both bathymetric data and model simulations with platforms present (Figure 6), younger shelf-edge deltas appear to be more sporadic in their distribution, and we attribute this to the positioning of the platforms. However, wave activity may also play a role in restricting depocenters on the outer shelf and upper slope, and future work would benefit from a computational examination of two-way coupling between fluvial supply and wave activity.

5.2. Platform Control on Submarine Canyon Incision

Model simulations indicate that the carbonate platform structures exert first-order control on the morphological development of the submarine canyons in the Noggin region (Figure 7). Previous hypotheses which state that canyons are incised by the scouring action of lowstand turbidity currents (e.g., Baztan et al., 2005; Daly, 1936; Mulder et al., 2003; Popescu et al., 2004; Pratson & Coakley, 1996) are supported here. In the case of the Noggin region, turbidity flows are further pre-conditioned by both the steepness of the continental

slope and the steepness of the platforms. When the platforms are subaerially exposed during lowstands, stream power is increased, and erosion is enhanced. Thus, hyperpycnal conditions are favored at the shelf edge. This is consistent with the presence of outer neritic and reefal sediments in turbidites deposited within canyons in the region (Puga-Bernabéu et al., 2014; Webster et al., 2012). More broadly, this mechanism could help explain the occurrence of numerous small canyons on slopes adjacent to carbonate platforms, which have been observed both in ancient record (Mullins & Cook, 1986) and in other modern settings (e.g., the Bahamas; Mullins et al., 1984; Tournadour et al., 2017). Regarding the influence of retrogressive erosion suggested by others (Puga-Bernabéu et al., 2013), our model does not explicitly capture this process, and we therefore will not rule out its potential influence on canyon development, especially given the model's sensitivity to the initial amphitheater-like depressions in the initial topographic surface. However, our model does support the occurrence of a top-down canyon incision style (Baztan et al., 2005; Pratson & Coakley, 1996), where localized incision of pre-canyon rills on the steep upper slope promotes a positive feedback of subsequent failure and further incision within the developing canyon head.

The influence of the carbonate platforms on canyon formation is further supported by seismic evidence. Prior to the Great Barrier Reef's initiation, and thus prior to the construction of the carbonate platforms on the Queensland shelf (which Feary et al. estimated to be ~0.76–1.01 Ma based on seismic interpretation), broad paleovalleys and sigmoidal/progradational geometries are interpreted on the shelf edge and upper slope (Feary et al., 1993; Symonds et al., 1983). Symonds et al. (1983) describe widespread upper slope deposition at this time, which is consistent with relatively high outer shelf and slope sedimentation rates derived from sediment cores (Feary & Jarrard, 1993). This represents a style of sedimentation that is more consistent with the reciprocal model (Jervey, 1988; Posamentier et al., 1988; Posamentier & Vail, 1988), where sediments are deposited at or near base level. We are able to reproduce this style of sedimentation simply by removing the carbonate platforms from the simulation, where net deposition occurs on the slope rather than canyon incision. Following the Great Barrier Reef's initiation, signs of increased slope incision appear in observational data, where Feary et al. (1993) interpret canyon incision since at least 80 ka. Similarly, when carbonate platforms are present in the model, canyon incision occurs at lowstand. Given these findings, we infer that the age of the canyons, at least in their current, dendritic-like morphological form, is constrained by the age of the platforms (~600 ka). Nevertheless, the proposed age for these canyons still remains tentative and could be clarified by a more extensive three-dimensional seismic survey.

It is possible that canyon incision and maintenance continues during highstands in the central Great Barrier Reef region. This relatively recent activity is indicated both by the presence of carbonate-dominated turbidites at highstand (Puga-Bernabéu et al., 2014) and the presence of sediment waves located within the axes of the canyon heads, which are imaged in multibeam bathymetric data (Puga-Bernabéu et al., 2013). Highstand canyons have been described in the cool-water carbonate Gippsland Basin system in southern Australia (Mitchell et al., 2007), where it is speculated that increased production of shelf-derived carbonates cause more frequent triggering of erosive turbidity currents and sediment gravity flows within canyon heads. It is possible that canyon downcutting and incision is triggered by a similar mechanism of supply-driven failure and erosion in the Great Barrier Reef region, as carbonate sediment production peaks during highstands (Dunbar & Dickens, 2003a). In warm water carbonate-dominated settings, this mechanism may be a consequence of a process more broadly referred to as “highstand shedding” (Droxler & Schlager, 1985; Schlager et al., 1994). However, within our current model framework, highstand shedding is not currently accounted for. Nevertheless, this mechanism should be more rigorously explored in the future.

5.3. Surface Gravity Flows and Turbidite Deposition

The spatial distribution of the gravity deposits simulated in the model, which were primarily triggered by turbidity currents at lowstand, generally corresponds to the spatial distribution of the surface gravity deposits observed in backscatter imagery. However, the real and simulated deposits differ in several notable ways (Figure 8). Simulated flows extend outward into the axis of the Queensland Trough as the turbidite record suggests (Puga-Bernabéu et al., 2011; Watts et al., 1993), where upon initiation, stream power is heightened by steep carbonate platform topography and localization of rivers through gaps between platforms. Similar to the flows observed in backscatter imagery, simulated flows are deflected northward by the Queensland Trough, where the lack of development of any significant submarine fans is attributed to relatively low supply and the deepening geometry of the trough. However, backscatter imagery implies clustering of flows

toward the north, whereas the simulated flows occur fairly evenly throughout the domain where gaps between platforms are present. This discrepancy may be due to the fact that backscatter imagery is more indicative of coarser-grained (sand-gravel) deposits and/or disintegrative landslides (Puga-Bernabéu et al., 2011), which are not simulated here and are preconditioned by an additional suite of slope stability factors (the degree of consolidation, the presence weak layers, overburdening, etc.; Hampton et al., 1996). In the model, flows are more indicative of turbidite deposition triggered under hyperpycnal conditions at the mouths of rivers and streams. In addition to a spatial mismatch of deposits, there also appears to be a timing mismatch. So far, deep sea sediment cores from this region do not yield any definitive relationship between turbidite occurrence and sea level (Dunbar et al., 2000; Puga-Bernabéu et al., 2014; Watts et al., 1993; Webster et al., 2012). As stated in the above section, because turbidite sedimentation is primarily generated during lowstands in the model (Figure 8), there are likely other triggering processes (e.g., highstand shedding, disintegrative landslides, storm events, and seismicity) that are presently unaccounted for in simulations (Schlager et al., 1994). This is further reinforced by the lack of turbidite sedimentation in the simulation where platforms are absent, despite the prolonged record of basin turbidite deposition in a core which pre-dates the Great Barrier Reef (i.e., since the Miocene; Watts et al., 1993).

5.4. Limitations and Future Directions

While we mention finer-scale model shortcomings in the previous discussion sections and in Table 1, we address broader study limitations here. First, in the absence of three-dimensional seismic data, we make several assumptions when constructing the initial “pre-Holocene” and “platforms absent” topographic surfaces. Regarding the pre-Holocene surface, the shelf’s ability to store sediments at lowstand is predicated upon topographic complexity, which alters stream power and facilitates deposition. Given the numerous drowned platforms and topographic depressions imaged in two-dimensional seismic sections (Johnson & Searle, 1984; Symonds et al., 1983; Webster et al., 2018), we deem it reasonable to assume that the initial topography would have been sufficiently complex, even without more precise knowledge of the initial surface. Nevertheless, this should be tested if the relevant data are acquired. Similarly, while the initial “platforms absent” surface was artificial, our results are consistent with higher sedimentation rates and thicker isopach maps on the outer shelf and upper slope prior to the establishment of the platforms (Feary et al., 1993; Feary & Jarrard, 1993). This suggests that our approximation of the surface is robust, lending confidence to the conclusion that sediment transport under these circumstances would be less circuitous and unimpeded. This study would nonetheless benefit from a more substantial sensitivity analysis of the initial topographic surface.

Finally, in the interest of prioritizing the most important mechanisms, the study’s scope did not capture the full set of oceanographic, climatic, hydraulic, sedimentological, and biological factors (i.e., tidal currents, upwelling, wind-driven currents, variable precipitation, bar and levee deposition, heterogeneous grain size, and lithology) that may be responsible for the presentation of certain geomorphological features. Additionally, whereas this model deterministically simulates processes over geological timescales, margin environments are inherently stochastic, and higher-frequency/higher-energy events such as floods and cyclones may be important in forming certain features. Finally, it would be worthwhile to examine the impact of vegetation (e.g., paleo-mangrove swamps) on both sediment supply and lowstand sediment storage (Bostock et al., 2007; Grindrod et al., 1999). In acknowledging the potential importance of these other processes, computational models can always be improved to test new hypotheses in conjunction with observational data.

6. Conclusions

Using numerical simulations, we show that carbonate platform geometry on the Great Barrier Reef margin directly preconditions the formation of several key geomorphological features on the shelf, slope, and in the basin. To demonstrate this, we run model simulations both with carbonate platforms present and platforms absent in the initial topographic surface. Using a variety of observations from multibeam data, seismic sections, backscatter imagery, and sediment cores, we show that several features appear when platforms are present. However, their distribution and occurrence are not reproduced when platforms are removed. From these data-model comparisons, we propose several platform-mediated mechanisms that form specific features in the Noggin region (central Great Barrier Reef):

1. On the inner to mid-shelf, platforms reduce the stream power of lowstand rivers, facilitating mounding and deposition around local topographic highs (i.e., the exposed karstified hills) and within local topographic depressions. Mounds are further constructed and reworked by wave-driven longshore currents during the transgression.
2. On the outer shelf, lowstand rivers are re-routed and siphoned between gaps in the platforms. Rivers locally regain their stream power within these gaps, incising paleochannels through knickpoint retreat. Shelf-edge deltas are also deposited by a combination of fluvial sources and local knickpoint retreat.
3. On the slope, steep platform topography locally increases stream power at the outer shelf edge during lowstand, eroding sediments and triggering turbidity currents that incise submarine canyons. Dendritic canyon morphologies are reproduced only when platforms are present in simulations.
4. In the surrounding basin, platforms act as conduits for fluvial and shelf-derived sediments. Lowstand turbidites are deflected north-westward by the Queensland Trough. Submarine fans do not appear due to low supply and the deepening geometry of the Queensland Trough.

We also identify areas where observations and model simulations diverge, suggesting mechanisms that are presently unaccounted for but may be influential in shaping the margin's geomorphological features. Our study demonstrates that numerical simulations can provide crucial place-specific insight into processes that operate on continental margins, particularly when they are unaccounted for within conventional sequence stratigraphic models.

Acknowledgments

Thran was supported by the University of Sydney DBH Scholarship. Salles was supported by both the ARC Training Centre in Data Analytics for Resources and Environments (DARE) and the ARC Research Hub for Basin GEodynamics and Evolution of Sedimentary Systems (GENESIS). Backscatter imagery was collected during a survey on the HMAS Cook, July 1989. Coastal background satellite imagery was provided with the backscatter imagery by the Australian Centre for Remote Sensing. Inland satellite imagery was provided by Google through the QGIS OpenLayers plug-in. The version of pyBadlands used in this study can be found online (zenodo.org/badge/latestdoi/192655024). The seismic boomer profile displayed in Figure 55a was reproduced under a CC BY 4.0 Creative Commons license (<http://creativecommons.org/licenses/by/4.0/legalcode>), where it was originally published by a predecessor of Geoscience Australia. This work was supported by Pawsey through the use of advanced computing resources. We thank Stephen Gallagher, Xiaoping Yuan, and editor Peter van der Beek for their careful and constructive reviews, which greatly improved the quality of the manuscript.

References

Abbey, E., Webster, J. M., & Beaman, R. J. (2011). Geomorphology of submerged reefs on the shelf edge of the Great Barrier Reef: The influence of oscillating Pleistocene sea-levels. *Marine Geology*, 288(1), 61–78. <https://doi.org/10.1016/j.margeo.2011.08.006>

Australian Bureau of Meteorology (2001). Map of climate zones of Australia. Melbourne, Australia: Commonwealth of Australia. Retrieved November 13, 2019, from www.bom.gov.au/climate/how/newproducts/images/zones.shtml

Australian Bureau of Meteorology (2019). Decadal and multi-decadal rainfall. Melbourne, Australia: Commonwealth of Australia. Retrieved from http://www.bom.gov.au/jsp/ncc/climate_averages/rainfall/index.jsp

Baztan, J., Berné, S., Olivet, J. L., Rabineau, M., Aslanian, D., Gaudin, M., et al. (2005). Axial incision: The key to understand submarine canyon evolution (in the western Gulf of Lion). *Marine and Petroleum Geology*, 22(6-7), 805–826. <https://doi.org/10.1016/j.marpetgeo.2005.03.011>

Beaman, R. J. (2010). Project 3D-GBR: A high-resolution depth model for the Great Barrier Reef and Coral Sea. Cairns, Australia: Project 2.5i.1a Final Report, Marine and Tropical Sciences Research Facility. Retrieved from <https://www.deeppref.org/bathymetry/65--3dgr-bathy.html>

Belperio, A. P. (1979). The combined use of wash load and bed material load rating curves for the calculation of total load: An example from the Burdekin River, Australia. *CATENA*, 6(3-4), 317–329. [https://doi.org/10.1016/0341-8162\(79\)90027-4](https://doi.org/10.1016/0341-8162(79)90027-4)

Bostock, H. C., Brooke, B. P., Ryan, D. A., Hancock, G., Pietsch, T., Packett, R., & Harle, K. (2007). Holocene and modern sediment storage in the subtropical macrotidal Fitzroy River estuary, Southeast Queensland, Australia. *Sedimentary Geology*, 201(3-4), 321–340. <https://doi.org/10.1016/j.sedgeo.2007.07.001>

Braithwaite, C. J. R., Dalmasso, H., Gilmour, M. A., Harkness, D. D., Henderson, G. M., Kay, R. L. F., et al. (2004). The Great Barrier Reef: The chronological record from a New Borehole. *Journal of Sedimentary Research*, 74(2), 298–310. <https://doi.org/10.1306/091603740298>

Braun, J., Heimsath, A. M., & Chappell, J. (2001). Sediment transport mechanisms on soil-mantled hillslopes. *Geology*, 29(8), 683–686. [https://doi.org/10.1130/0091-7613\(2001\)029<0683:STMSM>2.0.CO;2](https://doi.org/10.1130/0091-7613(2001)029<0683:STMSM>2.0.CO;2)

Bridge, T. C. L., Done, T. J., Friedman, A., Beaman, R. J., Williams, S. B., Pizarro, O., & Webster, J. M. (2011). Variability in mesophotic coral reef communities along the Great Barrier Reef, Australia. *Marine Ecology Progress Series*, 428, 63–75. <https://doi.org/10.3354/meps09046>

Brodie, J., Waterhouse, J., Lewis, S., Bainbridge, Z., & Johnson, J. (2009). Current loads of priority pollutants discharged from Great Barrier Reef Catchments to the Great Barrier Reef. Townsville, Australia: ACTFR Report 9.02, Australian Centre for Tropical Freshwater Research.

Burrows, M. A., Heijnis, H., Gadd, P., & Haberle, S. G. (2016). A new late Quaternary palaeohydrological record from the humid tropics of northeastern Australia. *Palaeogeography, Palaeoclimatology, Palaeoecology*, 451, 164–182. <https://doi.org/10.1016/j.palaeo.2016.03.003>

Carson, M. A., & Kirkby, M. J. (1972). *Hillslope form and process*. New York: Cambridge University Press.

Carter, R. M., Johnson, D. P., & Hooper, K. G. (1993). Episodic post-glacial sea-level rise and the sedimentary evolution of a tropical continental embayment (Cleveland Bay, Great Barrier Reef shelf, Australia). *Australian Journal of Earth Sciences*, 40(3), 229–255. <https://doi.org/10.1080/08120099308728077>

Daly, R. A. (1936). Origin of submarine canyons. *American Journal of Science*, 31(186), 401–420. <https://doi.org/10.2475/ajs.s5-31.186.401>

Davies, P. J., & Marshall, J. F. (1980). A model of epicontinental reef growth. *Nature*, 287, 37–38. <https://doi.org/10.1038/287037a0>

Davies, P. J., & McKenzie, J. A. (1993). Controls on the Pliocene–Pleistocene evolution of the northeastern Australian continental margin. In *Proceedings of the Ocean Drilling Program, Scientific Results*, (Vol. 133, pp. 755–762). College Station: TX (Ocean Drilling Program).

Davies, P. J., Symonds, P. A., Feary, D. A., & Pigram, C. J. (1989). The evolution of the carbonate platforms of northeast Australia. In P. D. Crevello, J. L. Wilson, J. F. Sarg, & J. F. Read (Eds.), *Controls on Carbonate Platforms and Basin Development* (Vol. 44, pp. 233–258). Special Publications of the Society of Economic Paleontologists and Mineralogists.

Department of Natural Resources and Mines. (2009). Drainage basins Queensland. Queensland Government. Retrieved from <http://qldspatial.information.qld.gov.au/catalogue/custom/detail.page?fid=%7BF79B22E5-7BD4-44AF-98EB-AC1A46513EDD%7D>

Dietrich, W. E., Reiss, R., Hsu, M.-L., & Montgomery, D. R. (1995). A process-based model for colluvial soil depth and shallow landsliding using digital elevation data. *Hydrological Processes*, 9(3–4), 383–400. <https://doi.org/10.1002/hyp.3360090311>

- Droxler, A. W., & Schlager, W. (1985). Glacial versus interglacial sedimentation rates and turbidite frequency in the Bahamas. *Geology*, 13(11), 799–802. [https://doi.org/10.1130/0091-7613\(1985\)13<799:GVISRA>2.0.CO;2](https://doi.org/10.1130/0091-7613(1985)13<799:GVISRA>2.0.CO;2)
- Dubois, N., Kindler, P., Spezzaferri, S., & Coric, S. (2008). The initiation of the southern central Great Barrier Reef: New multiproxy data from Pleistocene distal sediments from the Marion Plateau (NE Australia). *Marine Geology*, 250(3–4), 223–233. <https://doi.org/10.1016/j.margeo.2008.01.007>
- Dunbar, G. B., & Dickens, G. R. (2003a). Late Quaternary shedding of shallow-marine carbonate along a tropical mixed siliciclastic-carbonate shelf: Great Barrier Reef, Australia. *Sedimentology*, 50(6), 1061–1077. <https://doi.org/10.1046/j.1365-3091.2003.00593.x>
- Dunbar, G. B., & Dickens, G. R. (2003b). Massive siliciclastic discharge to slopes of the Great Barrier Reef Platform during sea-level transgression: Constraints from sediment cores between 15°S and 16°S latitude and possible explanations. *Sedimentary Geology*, 162(1–2), 141–158. [https://doi.org/10.1016/S0037-0738\(03\)00216-1](https://doi.org/10.1016/S0037-0738(03)00216-1)
- Dunbar, G. B., Dickens, G. R., & Carter, R. M. (2000). Sediment flux across the Great Barrier Reef Shelf to the Queensland Trough over the last 300 ky. *Sedimentary Geology*, 133(1), 49–92. [https://doi.org/10.1016/S0037-0738\(00\)00027-0](https://doi.org/10.1016/S0037-0738(00)00027-0)
- Durrant, T., Greenslade, D., Hemer, M., & Trenham, C. (2014). A global wave hindcast focussed on the Central and South Pacific. Melbourne, Australia: Australian Bureau of Meteorology. CAWCR Technical Report No. 070. http://www.cawcr.gov.au/publications/technicalreports/CTR_070.pdf
- Eberli, G. P., & Ginsburg, R. N. (1989). Cenozoic progradation of northwestern Great Bahama Bank, a record of lateral platform growth and sea-level fluctuations. In P. D. Crevello, J. L. Wilson, J. F. Sarg, & J. F. Read (Eds.), *Controls on carbonate platforms and basin development* (Vol. 44, pp. 339–355). Special Publications of the Society of Economic Paleontologists and Mineralogists.
- Emery, D., & Myers, K. (2009). *Sequence stratigraphy*. Hoboken, NJ: John Wiley & Sons.
- Fagherazzi, S., Howard, A. D., & Wiberg, P. L. (2004). Modeling fluvial erosion and deposition on continental shelves during sea level cycles. *Journal of Geophysical Research*, 109, F03010. <https://doi.org/10.1029/2003JF000091>
- Feary, D. A., & Jarrard, R. D. (1993). Sedimentology and downhole log analysis of Site 820, Central Great Barrier Reef outer shelf: The factors controlling Pleistocene Progradational and aggradational seismic geometry. In *Proceedings of the Ocean Drilling Program, Scientific Results*, (Vol. 133, pp. 315–326). College Station, TX: Ocean Drilling Program.
- Feary, D. A., Symonds, P. A., Davies, P. J., Pigram, C. J., & Jarrard, R. D. (1993). Geometry of Pleistocene facies on the Great Barrier Reef outer shelf and upper slope—Seismic stratigraphy of Sites 819, 820, and 821. In *Proceedings of the Ocean Drilling Program, Scientific Results*, (Vol. 133, pp. 327–351). College Station, TX: Ocean Drilling Program.
- Fielding, C. R., Trueman, J. D., Dickens, G. R., & Page, M. (2003). Anatomy of the buried Burdekin River channel across the Great Barrier Reef shelf: How does a major river operate on a tropical mixed siliciclastic/carbonate margin during sea level lowstand? *Sedimentary Geology*, 157(3–4), 291–301. [https://doi.org/10.1016/S0037-0738\(02\)00238-5](https://doi.org/10.1016/S0037-0738(02)00238-5)
- Fielding, C. R., Trueman, J. D., Dickens, G. R., & Page, M. (2005). Geomorphology and internal architecture of the Ancestral Burdekin River across the Great Barrier Reef Shelf, North-East Australia. In I. Jarvis, M. D. Blum, S. B. Marriott, & S. F. Leclair (Eds.), *Fluvial Sedimentology VII*, (pp. 321–347). Lincoln, Nebraska: Wiley. <https://doi.org/10.1002/9781444304350.ch18>
- Francis, J. M., Dunbar, G. B., Dickens, G. R., Sutherland, I. A., & Droxler, A. W. (2007). Siliciclastic sediment across the North Queensland Margin (Australia): A Holocene perspective on reciprocal versus coeval deposition in tropical mixed siliciclastic-carbonate systems. *Journal of Sedimentary Research*, 77(7), 572–586. <https://doi.org/10.2110/jsr.2007.057>
- Gallagher, S. J., Wallace, M. W., Hoiles, P. W., & Southwood, J. M. (2014). Seismic and stratigraphic evidence for reef expansion and onset of aridity on the Northwest Shelf of Australia during the Pleistocene. *Marine and Petroleum Geology*, 57, 470–481. <https://doi.org/10.1016/j.marpetgeo.2014.06.011>
- Gallop, S. L., Young, I. R., Ranasinghe, R., Durrant, T. H., & Haigh, I. D. (2014). The large-scale influence of the Great Barrier Reef matrix on wave attenuation. *Coral Reefs*, 33(4), 1167–1178. <https://doi.org/10.1007/s00338-014-1205-7>
- Goodwin, I. D. (2005). A mid-shelf, mean wave direction climatology for southeastern Australia, and its relationship to the El Niño—Southern Oscillation since 1878 A.D. *International Journal of Climatology*, 25(13), 1715–1729. <https://doi.org/10.1002/joc.1207>
- Grant, K. M., Rohling, E. J., Ramsey, C. B., Cheng, H., Edwards, R. L., Florindo, F., et al. (2014). Sea-level variability over five glacial cycles. *Nature Communications*, 5(1), 5076. <https://doi.org/10.1038/ncomms6076>
- Grindrod, J., Moss, P., & Van Der Kaars, S. (1999). Late Quaternary cycles of mangrove development and decline on the north Australian continental shelf. *Journal of Quaternary Science*, 14(5), 465–470. [https://doi.org/10.1002/\(SICI\)1099-1417\(199908\)14:5<465::AID-JQS473>3.0.CO;2-E](https://doi.org/10.1002/(SICI)1099-1417(199908)14:5<465::AID-JQS473>3.0.CO;2-E)
- Hampton, M. A., Lee, H. J., & Locat, J. (1996). Submarine landslides. *Reviews of Geophysics*, 34(1), 33–59. <https://doi.org/10.1029/95RG03287>
- Harris, P. T., Davies, P. J., & Marshall, J. F. (1990). Late Quaternary sedimentation on the Great Barrier Reef continental shelf and slope east of Townsville, Australia. *Marine Geology*, 94(1–2), 55–77. [https://doi.org/10.1016/0025-3227\(90\)90103-Q](https://doi.org/10.1016/0025-3227(90)90103-Q)
- Harris, P. T., Heap, A., Passlow, V., Hughes, M., Daniell, J., Hemer, M., & Anderson, O. (2005). Tidally incised valleys on tropical carbonate shelves: An example from the northern Great Barrier Reef, Australia. *Marine Geology*, 220(1–4), 181–204. <https://doi.org/10.1016/j.margeo.2005.06.019>
- Hinestrosa, G., Webster, J. M., & Beaman, R. J. (2016). Postglacial sediment deposition along a mixed carbonate-siliciclastic margin: New constraints from the drowned shelf-edge reefs of the Great Barrier Reef, Australia. *Palaeogeography, Palaeoclimatology, Palaeoecology*, 446, 168–185. <https://doi.org/10.1016/j.palaeo.2016.01.023>
- Hopley, D., Smithers, S. G., & Parnell, K. (2007). *The geomorphology of the Great Barrier Reef: Development, diversity and change*. Cambridge: Cambridge University Press. <https://doi.org/10.1017/CBO9780511535543>
- Howard, A. D. (1980). Thresholds in river regimes. In D. R. Coates, & J. D. Vitek (Eds.), *Thresholds in geomorphology*, (Vol. 227, pp. 227–258). Winchester, Mass: Allen and Unwin.
- Hughes, K., & Croke, J. (2017). How did rivers in the wet tropics (NE Queensland, Australia) respond to climate changes over the past 30 000 years? *Journal of Quaternary Science*, 32(6), 744–759. <https://doi.org/10.1002/jqs.2956>
- International Consortium for Great Barrier Reef Drilling, Alexander, I., Andres, M. S., Braithwaite, C. J. R., Braga, J. C., Davies, P. J., et al. (2001). New constraints on the origin of the Australian Great Barrier Reef: Results from an international project of deep coring. *Geology*, 29(6), 483–486. [https://doi.org/10.1130/0091-7613\(2001\)029<0483:NCOTOO>2.0.CO;2](https://doi.org/10.1130/0091-7613(2001)029<0483:NCOTOO>2.0.CO;2)
- Jervey, M. T. (1988). Quantitative geological modeling of siliciclastic rock sequences and their seismic expression. In C. K. Wilgus, B. S. Hastings, H. Posamentier, J. van Wagoner, C. A. Ross, & C. G. S. C. Kendall (Eds.), *Sea-level changes: An integrated approach* (Vol. 42, pp. 47–69). Tulsa, Oklahoma: Special Publications of the Society of Economic Paleontologists and Mineralogists.
- Johnson, D. P., & Searle, D. E. (1984). Post-glacial seismic stratigraphy, central Great Barrier Reef, Australia. *Sedimentology*, 31(3), 335–352. <https://doi.org/10.1111/j.1365-3091.1984.tb00863.x>

- Johnson, D. P., Searle, D. E., & Hopley, D. (1982). Positive relief over buried post-glacial channels, Great Barrier Reef Province, Australia. *Marine Geology*, 46(1-2), 149–159. [https://doi.org/10.1016/0025-3227\(82\)90156-6](https://doi.org/10.1016/0025-3227(82)90156-6)
- Jordan, T. E., & Flemings, P. B. (1991). Large-scale stratigraphic architecture, eustatic variation, and unsteady tectonism: A theoretical evaluation. *Journal of Geophysical Research*, 96(B4), 6681–6699. <https://doi.org/10.1029/90JB01399>
- Kendall, C. G. S. C., & Schlager, W. (1981). Carbonates and relative changes in sea level. *Marine Geology*, 44(1–2), 181–212. [https://doi.org/10.1016/0025-3227\(81\)90118-3](https://doi.org/10.1016/0025-3227(81)90118-3)
- Kolla, V., & Macurda, D. B. J. (1988). Sea-level changes and timing of turbidity-current events in deep-sea fan systems. In C. K. Wilgus, B. S. Hastings, H. Posamentier, J. Van Wagoner, C. A. Ross, & C. G. S. C. Kendall (Eds.), *Sea-level changes: An integrated approach, Special Publication* (Vol. 42, pp. 71–108). Tulsa, Oklahoma: Society of Economic Paleontologists and Mineralogists. Special Publications of SEPM.
- Lague, D., Hovius, N., & Davy, P. (2005). Discharge, discharge variability, and the bedrock channel profile. *Journal of Geophysical Research*, 110, F04006 <https://doi.org/10.1029/2004JF000259>
- Larcombe, P., Ridd, P. V., Prytz, A., & Wilson, B. (1995). Factors controlling suspended sediment on inner-shelf coral reefs, Townsville, Australia. *Coral Reefs*, 14(3), 163–171. <https://doi.org/10.1007/BF00367235>
- Lowe, D. R. (1976). Grain flow and grain flow deposits. *Journal of Sedimentary Research*, 46(1), 188–199. <https://doi.org/10.1306/212F6EF1-2B24-11D7-8648000102C1865D>
- Marshall, J. F., & Davies, P. J. (1982). Internal structure and Holocene evolution of One Tree Reef, southern Great Barrier Reef. *Coral Reefs*, 1, 21–28. <https://doi.org/10.1007/BF00286536>
- Marshall, J. F., & Davies, P. J. (1984). Last interglacial reef growth beneath modern reefs in the southern Great Barrier Reef. *Nature*, 307(5946), 44–46. <https://doi.org/10.1038/307044a0>
- Martin, Y., & Church, M. (1997). Diffusion in landscape development models: On the nature of basic transport relations. *Earth Surface Processes and Landforms: The Journal of The British Geomorphological Group*, 22(3), 273–279. [https://doi.org/10.1002/\(SICI\)1096-9837\(199703\)22:3<273::AID-ESP755>3.0.CO;2-D](https://doi.org/10.1002/(SICI)1096-9837(199703)22:3<273::AID-ESP755>3.0.CO;2-D)
- Maxwell, W. G. H., & Swinchatt, J. P. (1970). Great Barrier Reef: Regional variation in a terrigenous-carbonate province. *GSA Bulletin*, 81(3), 691–724. [https://doi.org/10.1130/0016-7606\(1970\)81\[691:GBRRVI\]2.0.CO;2](https://doi.org/10.1130/0016-7606(1970)81[691:GBRRVI]2.0.CO;2)
- Mitchell, J. K., Holdgate, G. R., Wallace, M. W., & Gallagher, S. J. (2007). Marine geology of the Quaternary Bass Canyon system, southeast Australia: A cool-water carbonate system. *Marine Geology*, 237(1-2), 71–96. <https://doi.org/10.1016/j.margeo.2006.10.037>
- Montaggioni, L. F. (2005). History of Indo-Pacific coral reef systems since the last glaciation: Development patterns and controlling factors. *Earth-Science Reviews*, 71(1-2), 1–75. <https://doi.org/10.1016/j.earscirev.2005.01.002>
- Moss, P. T., & Kershaw, A. P. (2007). A late Quaternary marine palynological record (oxygen isotope stages 1 to 7) for the humid tropics of northeastern Australia based on ODP Site 820. *Palaeogeography, Palaeoclimatology, Palaeoecology*, 251(1), 4–22. <https://doi.org/10.1016/j.palaeo.2007.02.014>
- Mount, J. F. (1984). Mixing of siliciclastic and carbonate sediments in shallow shelf environments. *Geology*, 12(7), 432–435. [https://doi.org/10.1130/0091-7613\(1984\)12<432:MOSACS>2.0.CO;2](https://doi.org/10.1130/0091-7613(1984)12<432:MOSACS>2.0.CO;2)
- Mulder, T., Syvitski, J. P. M., Migeon, S., Faugères, J.-C., & Savoye, B. (2003). Marine hyperpycnal flows: Initiation, behavior and related deposits. A review. *Marine and Petroleum Geology*, 20(6-8), 861–882. <https://doi.org/10.1016/j.marpetgeo.2003.01.003>
- Mullins, H. T., & Cook, H. E. (1986). Carbonate apron models: Alternatives to the submarine fan model for paleoenvironmental analysis and hydrocarbon exploration. *Sedimentary Geology*, 48(1-2), 37–79. [https://doi.org/10.1016/0037-0738\(86\)90080-1](https://doi.org/10.1016/0037-0738(86)90080-1)
- Mullins, H. T., Heath, K. C., van Buren, H. M., & Newton, C. R. (1984). Anatomy of a modern open-ocean carbonate slope: Northern Little Bahama Bank. *Sedimentology*, 31(2), 141–168. <https://doi.org/10.1111/j.1365-3091.1984.tb01956.x>
- Neil, D. T., Orpin, A. R., Ridd, P. V., & Yu, B. (2002). Sediment yield and impacts from river catchments to the Great Barrier Reef lagoon: A review. *Marine and Freshwater Research*, 53(4), 733–752. <https://doi.org/10.1071/MF00151>
- O’Callaghan, J. F., & Mark, D. M. (1984). The extraction of drainage networks from digital elevation data. *Computer Vision, Graphics, and Image Processing*, 28(3), 323–344. [https://doi.org/10.1016/S0734-189X\(84\)80011-0](https://doi.org/10.1016/S0734-189X(84)80011-0)
- Orme, G. R., Webb, J. P., Kelland, N. C., & Sargent, G. E. G. (1978). Aspects of the geological history and structure of the northern Great Barrier Reef. *Philosophical Transactions of the Royal Society of London. Series A, Mathematical and Physical Sciences*, 291(1378), 23–35. <https://doi.org/10.1098/rsta.1978.0087>
- Orpin, A. R., Brunskill, G. J., Zagorskis, I., & Woolfe, K. J. (2004). Patterns of mixed siliciclastic-carbonate sedimentation adjacent to a large dry-tropics river on the central Great Barrier Reef shelf, Australia. *Australian Journal of Earth Sciences*, 51(5), 665–683. <https://doi.org/10.1111/j.1400-0952.2004.01083.x>
- Page, M. C., & Dickens, G. R. (2005). Sediment fluxes to Marion Plateau (southern Great Barrier Reef province) over the last 130 ky: New constraints on ‘transgressive-shedding’ off northeastern Australia. *Marine Geology*, 219(1), 27–45. <https://doi.org/10.1016/j.margeo.2005.05.002>
- Page, M. C., Dickens, G. R., & Dunbar, G. B. (2003). Tropical view of Quaternary sequence stratigraphy: Siliciclastic accumulation on slopes east of the Great Barrier Reef since the Last Glacial Maximum. *Geology*, 31(11), 1013–1016. <https://doi.org/10.1130/G19622.1>
- Petit, C., Migeon, S., & Coste, M. (2015). Numerical models of continental and submarine erosion: Application to the northern Ligurian Margin (Southern Alps, France/Italy). *Earth Surface Processes and Landforms*, 40(5), 681–695. <https://doi.org/10.1002/esp.3685>
- Planchon, O., & Darboux, F. (2002). A fast, simple and versatile algorithm to fill the depressions of digital elevation models. *CATENA*, 46(2-3), 159–176. [https://doi.org/10.1016/S0341-8162\(01\)00164-3](https://doi.org/10.1016/S0341-8162(01)00164-3)
- Popescu, I., Lericolais, G., Panin, N., Normand, A., Dinu, C., & Le Drenzen, E. (2004). The Danube submarine canyon (Black Sea): Morphology and sedimentary processes. *Marine Geology*, 206(1-4), 249–265. <https://doi.org/10.1016/j.margeo.2004.03.003>
- Posamentier, H. W., Jervey, M. T., & Vail, P. R. (1988). Eustatic controls on clastic deposition I—conceptual framework. In C. K. Wilgus, B. S. Hastings, C. G. S. C. Kendall, H. W. Posamentier, C. A. Ross, & J. C. Van Wagoner (Eds.), *Sea level changes: An integrated approach* (Vol. 42, pp. 109–124). Special Publications of the Society of Economic Paleontologists and Mineralogists.
- Posamentier, H. W., & Vail, P. R. (1988). Eustatic controls on clastic deposition II—Sequence and systems tract models. In C. K. Wilgus, B. S. Hastings, C. G. S. C. Kendall, H. W. Posamentier, C. A. Ross, & J. C. Van Wagoner (Eds.), *Sea level changes: An integrated approach* (Vol. 42, pp. 125–154). Special Publications of the Society of Economic Paleontologists and Mineralogists.
- Pratson, L. F., & Coakley, B. J. (1996). A model for the headward erosion of submarine canyons induced by downslope-eroding sediment flows. *GSA Bulletin*, 108(2), 225–234. [https://doi.org/10.1130/0016-7606\(1996\)108<0225:AMFTHE>2.3.CO;2](https://doi.org/10.1130/0016-7606(1996)108<0225:AMFTHE>2.3.CO;2)
- Pratson, L. F., Nittrouer, C. A., Wiberg, P. L., Steckler, M. S., Swenson, J. B., Cacchione, D. A., et al. (2007). Seascape evolution on clastic continental shelves and slopes. In C. A. Nittrouer, J. A. Austin, M. E. Field, J. H. Kravitz, J. P. M. Syvitski, & P. L. Wiberg (Eds.),

- Continental margin sedimentation: From sediment transport to sequence stratigraphy*, (pp. 339–380). Hoboken, NJ: Wiley. <https://doi.org/10.1002/9781444304398.ch7>
- Puga-Bernabéu, Á., Webster, J. M., Beaman, R. J., & Guilbaud, V. (2011). Morphology and controls on the evolution of a mixed carbonate-siliciclastic submarine canyon system, Great Barrier Reef margin, north-eastern Australia. *Marine Geology*, 289(1-4), 100–116. <https://doi.org/10.1016/j.margeo.2011.09.013>
- Puga-Bernabéu, Á., Webster, J. M., Beaman, R. J., & Guilbaud, V. (2013). Variation in canyon morphology on the Great Barrier Reef margin, north-eastern Australia: The influence of slope and barrier reefs. *Geomorphology*, 191, 35–50. <https://doi.org/10.1016/j.geomorph.2013.03.001>
- Puga-Bernabéu, Á., Webster, J. M., Beaman, R. J., Reimer, P. J., & Renema, W. (2014). Filling the gap: A 60 ky record of mixed carbonate-siliciclastic turbidite deposition from the Great Barrier Reef. *Marine and Petroleum Geology*, 50, 40–50. <https://doi.org/10.1016/j.marpetgeo.2013.11.009>
- Rasmussen, E. S. (1994). The relationship between submarine canyon fill and sea-level change: An example from Middle Miocene offshore Gabon, West Africa. *Sedimentary Geology*, 90(1-2), 61–75. [https://doi.org/10.1016/0037-0738\(94\)90017-5](https://doi.org/10.1016/0037-0738(94)90017-5)
- Ryan, D. A., Bostock, H. C., Brooke, B. P., & Marshall, J. F. (2007). Bathymetric expression of the Fitzroy River palaeochannel, northeast Australia: Response of a major river to sea-level change on a semi-rimmed, mixed siliciclastic-carbonate shelf. *Sedimentary Geology*, 201(1-2), 196–211. <https://doi.org/10.1016/j.sedgeo.2007.05.018>
- Ryan, D. A., Brooke, B. P., Bostock, H. C., Radke, L. C., Siwabessy, P. J. W., Margvelashvili, N., & Skene, D. (2007). Bedload sediment transport dynamics in a macrotidal embayment, and implications for export to the southern Great Barrier Reef shelf. *Marine Geology*, 240(1-4), 197–215. <https://doi.org/10.1016/j.margeo.2007.02.014>
- Salles, T., Ding, X., & Brocard, G. (2018). pyBadlands: A framework to simulate sediment transport, landscape dynamics and basin stratigraphic evolution through space and time. *PLoS ONE*, 13(4). <https://doi.org/10.1371/journal.pone.0195557>
- Salles, T., Ding, X., Webster, J. M., Vila-Concejo, A., Brocard, G., & Pall, J. (2018). A unified framework for modelling sediment fate from source to sink and its interactions with reef systems over geological times. *Scientific Reports*, 8(1), 5252. <https://doi.org/10.1038/s41598-018-23519-8>
- Salles, T., & Hardiman, L. (2016). Badlands: An open-source, flexible and parallel framework to study landscape dynamics. *Computers & Geosciences*, 91, 77–89. <https://doi.org/10.1016/j.cageo.2016.03.011>
- Sarg, J. F. (1988). Carbonate sequence stratigraphy. In C. K. Wilgus, B. S. Hastings, C. A. Ross, H. Posamentier, J. Van Wagoner, & C. G. S. Kendall (Eds.), *Sea level changes—An integrated approach* (Vol. 42, pp. 155–181). Special Publications of the Society of Economic Paleontologists and Mineralogists.
- Saunders, I., & Young, A. (1983). Rates of surface processes on slopes, slope retreat and denudation. *Earth Surface Processes and Landforms*, 8(5), 473–501. <https://doi.org/10.1002/esp.3290080508>
- Schlager, W., & Adams, E. W. (2001). Model for the sigmoidal curvature of submarine slopes. *Geology*, 29(10), 883–886. [https://doi.org/10.1130/0091-7613\(2001\)029<0883:MFTSCO>2.0.CO;2](https://doi.org/10.1130/0091-7613(2001)029<0883:MFTSCO>2.0.CO;2)
- Schlager, W., Reijmer, J. J. G., & Droxler, A. (1994). Highstand shedding of carbonate platforms. *Journal of Sedimentary Research*, 64(3b), 270–281. <https://doi.org/10.1306/D4267FAA-2B26-11D7-8648000102C1865D>
- Shulmeister, J., & Lees, B. G. (1995). Pollen evidence from tropical Australia for the onset of an ENSO-dominated climate at c. 4000 BP. *The Holocene*, 5(1), 10–18. <https://doi.org/10.1177/095968369500500102>
- Sumner, G., & Bonell, M. (1986). Circulation and daily rainfall in the North Queensland wet seasons 1979–1982. *Journal of Climatology*, 6(5), 531–549. <https://doi.org/10.1002/joc.3370060507>
- Sweeney, K. E., Roering, J. J., & Ellis, C. (2015). Experimental evidence for hillslope control of landscape scale. *Science*, 349(6243), 51–53. <https://doi.org/10.1126/science.aab0017>
- Symonds, P. A., Davies, P. J., & Parisi, A. (1983). Structure and stratigraphy of the central Great Barrier Reef. *BMR Journal of Australian Geology and Geophysics*, 8(3), 277–291.
- Tournadour, E., Mulder, T., Borgomano, J., Gillet, H., Chabaud, L., Ducassou, E., et al. (2017). Submarine canyon morphologies and evolution in modern carbonate settings: The northern slope of Little Bahama Bank, Bahamas. *Marine Geology*, 391, 76–97. <https://doi.org/10.1016/j.margeo.2017.07.014>
- Tucker, G., Lancaster, S., Gasparini, N., & Bras, R. (2001). The Channel-Hillslope Integrated Landscape Development Model (CHILD). In R. S. Harmon, & W. W. Doe (Eds.), *Landscape Erosion and Evolution Modeling*, (pp. 349–388). Boston, MA: Springer US. https://doi.org/10.1007/978-1-4615-0575-4_12
- van Wagoner, J. C., Posamentier, H. W., Mitchum, R. M. J., Vail, P. R., Sarg, J. F., Loutit, T. S., & Hardenbol, J. (1988). An overview of the fundamentals of sequence stratigraphy and key definitions. In C. K. Wilgus, B. S. Hastings, C. A. Ross, H. Posamentier, J. Van Wagoner, & C. G. S. Kendall (Eds.), *Sea level changes: An integrated approach* (Vol. 42, pp. 39–45). Special Publications of the Society of Economic Paleontologists and Mineralogists.
- Watts, K. F., Varga, L. L., & Feary, D. A. (1993). Origins, timing, and implications of Miocene to Pleistocene turbidites, debris flows, and slump deposits of the Queensland Trough, northeastern Australia (Site 823). In *Proceedings of the Ocean Drilling Program, Scientific Results* (Vol. 133, pp. 379–445). College Station, TX: Ocean Drilling Program. <https://doi.org/10.2973/odp.proc.sr.133.248.1993>
- Webster, J. M., Beaman, R. J., Puga-Bernabéu, Á., Ludman, D., Renema, W., Wust, R. A., et al. (2012). Late Pleistocene history of turbidite sedimentation in a submarine canyon off the northern Great Barrier Reef, Australia. *Palaeogeography, Palaeoclimatology, Palaeoecology*, 331–332, 75–89. <https://doi.org/10.1016/j.palaeo.2012.02.034>
- Webster, J. M., Braga, J. C., Humblet, M., Potts, D. C., Iryu, Y., Yokoyama, Y., et al. (2018). Response of the Great Barrier Reef to sea-level and environmental changes over the past 30,000 years. *Nature Geoscience*, 11(6), 426–432. <https://doi.org/10.1038/s41561-018-0127-3>
- Webster, J. M., & Davies, P. J. (2003). Coral variation in two deep drill cores: Significance for the Pleistocene development of the Great Barrier Reef. *Sedimentary Geology*, 159(1-2), 61–80. [https://doi.org/10.1016/S0037-0738\(03\)00095-2](https://doi.org/10.1016/S0037-0738(03)00095-2)
- Webster, J. M., Davies, P. J., Beaman, R. J., Williams, S., & Byrne, M. (2008). Evolution of drowned shelf edge reefs in the GBR: Implications for understanding abrupt climate change, coral reef response and modern deep water benthic habitats (p. 18). Hobart, Tasmania: Marine National Facility. Retrieved from <http://www.marine.csiro.au/national-facility/voyagedocs/2007/summarySS07-2007.pdf>
- Whipple, K. X., & Tucker, G. E. (1999). Dynamics of the stream-power river incision model: Implications for height limits of mountain ranges, landscape response timescales, and research needs. *Journal of Geophysical Research*, 104(B8), 17,661–17,674. <https://doi.org/10.1029/1999JB900120>
- Woolfe, K. J., Larcombe, P., Purdon, R. G., & Naish, T. (1998). Lowstand rivers need not incise the shelf: An example from the Great Barrier Reef, Australia, with implications for sequence stratigraphic models. *Geology*, 26(1), 75–78. [https://doi.org/10.1130/0091-7613\(1998\)026<0075:LRNNIT>2.3.CO;2](https://doi.org/10.1130/0091-7613(1998)026<0075:LRNNIT>2.3.CO;2)

- Yokoyama, Y., Esat, T. M., Thompson, W. G., Thomas, A. L., Webster, J. M., Miyairi, Y., et al. (2018). Rapid glaciation and a two-step sea level plunge into the Last Glacial Maximum. *Nature*, *559*(7715), 603–607. <https://doi.org/10.1038/s41586-018-0335-4>
- Zadeh, L. A. (1965). Fuzzy sets. *Information and Control*, *8*, 338–353.